Ensemble Generation For Hurricane Hazard Assessment Along The United States' Atlantic Coast

Abolfazl Hojjat Ansari[1], Mohammad Ali Olyaei[1], and Zahra Heydari[2]

[1]University of Tehran
[2]University of Illinois Urbana-Champaign

November 21, 2022

Abstract

Scarcity of available records is a major hindrance in hurricane hazard assessment. In addition, frequency analysis on maximum intensities of all historical storms is incapable of analyzing very rare phenomena. Ensemble generation is crucial for circumventing these difficulties, targeted at this study. We will show here that ensembles like Sandy can be statistically generated even by removing its trajectory from historical records. We began with historical compilations of NOAA National Climatic Data Center (NCDC) tropical cyclone (TC) database. TC reaching a hurricane strength and making landfall in or passing close to the United States were identified. The geographical area influenced by these hurricanes was discretized and the parameters of Markov chains and multivariate distributions were derived for each discretized area. Synthetic tracks were generated using repetitive random draws from the spatiotemporal distribution of historical genesis and storm motion, conditioned by Markov chains for each 6-hour displacement. The proposed algorithm is validated in macro and micro scales. In macro scale, tracks coming within the specified radius of an area of interest were counted for a given hurricane scale. The results revealed that the general pattern of hits conforms well to historical observations. In micro scale, the model was evaluated for Miami and New York City with quite different hurricane climatology. The track generator produces a history of potential wind and translational speeds for both of these regions as well.

Posted on 21 Nov 2022 — The copyright holder is the author/funder. All rights reserved. No reuse without permission. — https://doi.org/10.1002/essoar.10506370.1 — This a preprint and has not been peer reviewed. Data may be preliminary.

Ensemble Generation For Hurricane Hazard Assessment Along The United States' Atlantic Coast

A. Hojjat-Ansari[1], M. A. Olyaei[1], Zahra Heydari[2]

[1]School of Civil Engrg., College of Engrg., Univ. of Tehran, Tehran, Iran
[2]College of Civil and Environmental Engrg., Univ. of Illinois Urbana-Champaign, the United States

Key Points:

- The track generator produces the general pattern of hurricane hits, conforming to historical records.
- Ensembles can be generated in large numbers in areas that rarely experience severe storms, with the history of strengths and speeds.
- Ensembles of unique trajectories like hurricane Sandy can be reconstructed even by removing their trajectories from historical records.

Corresponding author: Abolfazl Hojjat Ansari, `rashid.hojjatansari@gmail.com`

Abstract

Scarcity of available records is a major hindrance in hurricane hazard assessment. In addition, frequency analysis on maximum intensities of all historical storms is incapable of analyzing very rare phenomena. Ensemble generation is crucial for circumventing these difficulties, targeted at this study. We will show here that ensembles like Sandy can be statistically generated even by removing its trajectory from historical records. We began with historical compilations of NOAA National Climatic Data Center (NCDC) tropical cyclone (TC) database. TC reaching a hurricane strength and making landfall in or passing close to the United States were identified. The geographical area influenced by these hurricanes was discretized and the parameters of Markov chains and multivariate distributions were derived for each discretized area. Synthetic tracks were generated using repetitive random draws from the spatiotemporal distribution of historical genesis and storm motion, conditioned by Markov chains for each 6-hour displacement. The proposed algorithm is validated in macro and micro scales. In macro scale, tracks coming within the specified radius of an area of interest were counted for a given hurricane scale. The results revealed that the general pattern of hits conforms well to historical observations. In micro scale, the model was evaluated for Miami and New York City with quite different hurricane climatology. The track generator produces a history of potential wind and translational speeds for both of these regions as well.

1 Introduction

Tropical cyclones (TCs), are one of the most catastrophic hydro-meteorological natural disasters in coastal environments (Varlas et al., 2018). These deadly disasters are associated with strong winds, heavy rainfall and large storm surges and account for a significant fraction of damage, injury and loss of life from natural hazards (Hoque et al., 2016; Puotinen, 2007). Since 1980, land falling hurricanes in the continental U.S. have caused two thirds of the global total damages from natural hazards (Mohleji & Pielke Jr, 2014; Weinkle et al., 2018). For example, in 2005, Hurricane Katrina known to be the most devastating disaster in the U.S. produced the highest flooding in the history of the U.S., resulting in more than USD120 billion in terms of damages and causing approximately 2000 mortalities. Similarly, damages and fatalities associated with Hurricanes Sandy in 2012; Harvey, Irma, and Maria in 2017, and Florence and Michael in 2018 have highlighted the power of hurricanes to cause destruction on even one of the most advanced societies (Emanuel et al., 2006; Freeman & Ashley, 2017; Garner et al., 2017; Lin et al., 2012, 2016; Reed et al., 2015; Shuckburgh et al., 2017). Being the costliest natural catastrophes in the US with nearly US 5 bilion dollars damage per year (Burroughs, 2007), a qualitatively appropriate assessment and an accurate prediction of tropical cyclone activity can never be overemphasized (Pielke Jr et al., 2008; Woodruff et al., 2013; Mei et al., 2019).

TCs are strong atmospheric perturbations which depending on their location and intensity, would range from hurricanes, typhoons, and tropical storm to cyclonic storms, tropical depressions and cyclones (NOAA, 2015). TCs usually form between 5 and 30-degree latitude away from the equator; the lower limit satisfies the minimum Coriolis force required to develop TCs (Gomes et al., 2015). As the TCs develops, there would be a transition point where it converts to an extratropical system in which the source of movement instead of latent heat relies on the so called "baroclinic instability" referring to the temperature contrast as a result of interaction of cold and warm air masses (Georgiev et al., 2016). Extratropical cyclones are usually accompanied with extreme rainfall and strong winds (Hawcroft et al., 2012)

TC activities can be characterized by various metrics, including annual frequency, tracks, maximum speed wind (MSW), translational velocity as well as life time duration (Emanuel, 2005). These characteristics are also the components for TC forecasting which directly affect specific hazards (e.g, surge inundation) experienced at vulnerable populations at locations with high exposure. Thus, the ability to conduct an accurate hazard assessment is of paramount importance, especially for vulnerable communities. Coastal regions suffer from this vulnerability the most as tropical cyclones normally weaken when moving landward with a cut-off from their original energy source; thus, due to lower translation speed, result in a longer passage time through a region, resulting in greater rainfall totals (Workgroup, 2015; Lam et al., 2017; Lai et al., 2020) and storm surge flooding. To mitigate these effects in vulnerable regions and improve preparedness, TC hazard assessments must be acceptably accurate and reliable (Villarini et al., 2019), which means sufficient observational data are an inevitable initiative.

For TCs, the scarcity of observational data, rarity of extreme events for each specific area of the North Atlantic which is the focus of this paper, and their often poor quality, has lead statistical analysis, on which hazard assessments heavily rely, to deal with these challenges by considering the uncertainties that lie within the track and intensity of a TC (Coles & Simiu, 2003; Hallegatte et al., 2007). Therefore, when considering the possibility of highly destructive events occurring in the future, the hazard assessment should be addressed through the use of probabilistic models which allow for the available information to be used in predicting potential catastrophic consequences. Accordingly, to grasp a reasonable understanding of the internal variability of TCs, hazard assessment methods usually rely on large ensembles of model simulations to make up for any shortness of data in characterizing cyclones tracks, intensities, and their consequential damaging effects (Done et al., 2014; Loridan et al., 2015; Mei et al., 2019).

Ensemble techniques are a relatively new approach, and proven to be vital, to probabilistic analysis. They are usually based on large sets of synthetic storm tracks and intensities generated from the statistics of historical tracks to lengthen the dataset needed for proper statistical analysis of the return periods of landfalling TCs (Vickery, 2005; Gneiting & Raftery, 2005; Yonekura & Hall, 2011; Bloemendaal et al., 2020). Ensemble members are stochastic realizations which mainly contribute to normalizing uncertainties associated with initial conditions.

Hurricane Risk Analysis is still an ongoing challenge aiming to reach a comprehensive approach to overcome data scarcity, shortness of data series, and other problematic estimations that rise from the uncertain nature of hurricanes. In most studies the statistics of the generated storms are either based on limited number of storms in a short period of time (Wooten & Tsokos, 2008), or not based on historical observations, but rather randomly generated in specific defined intervals (Gomes et al., 2015). While more recent studies tend to make up for the shortness of historical data through statistic resampling to generate track data, still, these generations are based on the average climate conditions of those limited years and therefore, cannot capture multi-decadal variability on longer time scales (Bloemendaal et al., 2020). Here, by extending the statistical analysis period between 1851 and 2017, we present an algorithm that can predict the path of storms that are likely to occur in the future and calculate the probability of such occurrence. The model results can be used as input to hydrodynamic models to assess flood risk in different areas of the US Atlantic coast.

The outline of this paper is as follows. First, the extraction of 2162 historical records over a 166-year period is explained, followed by a three step process (multivariate distribution, Markov chain, and transition) of hurricane ensemble (Section 2). Then, statistical assessments are presented in macro (the east coast of the U.S) and mini (for New York and Miami) scales in section 3.The paper ends with section 4, summarizing the main conclusions of this study and proposing future research direction.

2 Methodology

2.1 Hurricane data

Our algorithm begins with statistical compilations of historical records of North Atlantic hurricanes. Over the 166-year period 1851 through 2017, a total of 2162 tropical cyclones have been documented over the North Atlantic Basin. The geometry and intensity information of these tropical cyclones were extracted from the archive of NOAA National Climatic Data Center (NCDC) using 'rnoaa' R package (Edmund et al., 2014). These information so called "best track" data consist of a set of key variables, including latitude and longitude of trajectory (Lat and Lon), maximum sustained wind (MSW), and central pressure deficit (ΔP), which are frequently available at 6-hour intervals. These data were screened to remove missing values and adjust all time intervals to 6-hour. Central pressure deficit before 1975 has many missing values. However, the records of MSW is much more complete and we found a significant correlation (93%) between MSW and central pressure deficit, which allows for an acceptable approach to measure hurricane intensity only through MSW. Due to the destructive potential of hurricanes, reliable hazard assessment of these dynamical energy-deriven systems are of our interest. According to Saffir-Simpson scale (Taylor et al., 2010), the term hurricane is assigned to tropical cyclones that have MSW greater than 64 knots (118.5 km/h). Therefore, in order to synthesize storms that could pose a significant risk to coastal areas, tropical cyclones reaching hurricane strength during their life cycle were selected. Of the 503 hurricanes selected in this fashion, only 264 hurricanes made landfall in and/or passed close enough to the East Coast. The statistics of these 264 hurricanes were used to synthesize storm tracks and intensities that could potentially threaten the East Coast. Ancillary features including life cycle duration (D), translational velocity (V), and azimuth (ϕ) were characterized for these hurricanes based on their 6-hour positions through Equations 1 to 3, respectively.

$$D^j = T_n^j - T_1^j \tag{1}$$

$$V_i^j = \frac{distm(lon_{i-1}^j, lat_{i-1}^j, lon_i^j, lat_i^j)}{T_i^j - T_{i-1}^j} \tag{2}$$

$$\phi_i^j = bearing(lon_{i-1}^j, lat_{i-1}^j, lon_i^j, lat_i^j) \tag{3}$$

where D^j is the life cycle duration of j^{th} hurricane. V_i^j, ϕ_i^j, lon_i^j and lat_i^j represent translational velocity, azimuth, longitude, latitude of j^{th} hurricane at i^{th} interval, respectively. T_i^j is the time of j^{th} hurricane at i^{th} interval of its life cycle. T_1^j and T_n^j represent the time of beginning and end of j^{th} hurricane, respectively. distm() and bearing() calculates the distance and bearing between two geographic points, corresponding to functions available at 'geosphere' R package.

2.2 Study site

The formation of these hurricanes takes place in the Caribbean Sea, Gulf of Mexico, and westward off the coast of Africa between 5°N and 30°N latitude. The geographical area influenced by these 264 hurricanes, enclosed by 8°N and 45°N latitude and 15°W and 100°W longitude, was discretized into regions of A to H shown in Figure 1. Such a discretization was made for three reasons. First, the mutual correlation of hurricane features varies from region to region and therefore, dividing this area into smaller regions makes it possible to better model the mutual correlation of explanatory variables. Second, transformation of variables in this case is easier for further statistical analysis. Third, hurricanes may transition to extratropical state by passing 30°N latitude. Statistical modeling of this transition is provided by dividing the area at this latitude.

Figure 1. Geographical area influenced by the hurricanes that made landfall in the United States or passed close enough

2.3 Hurricane ensemble

2.3.1 Multivariate distribution

All hurricane features were classified based on their geographical position and assigned to each region. Following this classification, the data of each region was divided into genesis and storm motion data. The parameters of normal multivariate distribution for these two sets of data, then, were estimated separately.

The prerequisite for making a multi-variate normal distribution of several variables is the normality of the distribution of involving variables. However, most of these variables do not follow normal distribution, in particular, MSW is extremely right-skewed. Therefore, these variables need to be transformed into normal distribution. For this purpose, using 'bestNormalize' R package, various normalizing transformations including Box-Cox, Yeo-Johnson, ordered quantile normalization, Lambert WxF transformations and other commonly used transformations such as exponential and lognormal transformations were implemented on data sets and the best one was selected based on the goodness of fit statistic. To overcome the limitations of applying some normalizing transformations on negative data, the longitude values were transformed to positive ones and the azimuth values, which had been defined between the range of $-\pi$ and $+\pi$, were transformed to the range of $0°$ to $360°$. After normalizing the explanatory variables the mutual correlations of them were calculated in the form of covariance matrix, which was used along with mean vector to make the multivariate normal distributions of genesis in each region. With a similar process, normal multivariate distributions were made for the storm motion data in each zone for all variables except life cycle duration that was already set with the genesis.

2.3.2 Markov chain

MSW, translational velocity and azimuth were considered as sequential states of a random process whose states were determined in the next step based on their states in the previous steps. These variables vary in ranges from 0 to 165 knots, 0 to 42 m/s, and 0 to 360°, respectively, and differ from region to region. For defining variable states, MSWs were discretized at 10 knots, translational velocities at 2 m/s and azimuths at 20°, categorizing into 17, 18, and 22 possible states, respectively.

If $X = \{x_1, x_2, x_3, \ldots, x_n\}$ is a sequence of observations of a random process over time, and $S = \{s_1, s_2, \ldots, s_n\}$ is the states of this random process such that $X \in S$, then, based on the Markov chain formulation, the probability that the observation in n^{th} step being in s_n state is determined as follows:

$$P(x_n = s_n | x_1 = s_1, x_2 = s_2, \ldots, x_{n-1} = s_{n-1}) = P(x_n = s_n | x_{n-1} = s_{n-1}) \qquad (4)$$

According to Equation 4, the state of the process in n^{th} step depends only on the previous step, referred as lag-1 Markov model. Let s_i and s_j represent any two states; the conditional probabilities that the process moves to state s_j at time n, given it is in the state of s_i at time $n-1$, are determined as follows:

$$p_{ij} = P(x_n = s_j | x_{n-1} = s_i) \qquad (5)$$

where p_{ij} is the probability that the process moves from state s_i to state s_j in one time step.

In each discretized geographical area shown in Figure 1, transition probabilities were trained on historical records by counting transition between the different states and calculating their respective relative frequencies.

2.3.3 Transition

Like any other element of the climate system, TCs go through different stages in the course of a life cycle. They may lose their tropical characteristics after moving into a non-tropical environment and become extratropical. Such a transition from a tropical to an extratropical cyclone leads to a sudden change in the structure of the cyclone. Drastic variations in MSW, direction, and position are a result of this structural change. Figure 2 shows the position of such transitions, where each pair of the same color represents a hurricane in tropical (TS) and extratropical (ET) stages.

Figure 2. Historical recorded transition points. (same coloured points indicates a transition from tropical state (TS) to extratropical state (ET) for a hurricane)

According to this figure, Hurricane transition often occurs above 30°N latitude, i.e. regions H and I. Thus, unlike other regions where the storm is generally in the tropical state, in these two regions the storm either remains in the same stage; that is, $TS \rightarrow TS$ and $ET \rightarrow ET$, or transitions into extratropical system i.e. $TS \rightarrow ET$. Hence, we considered the transitional probabilities in these two regions based on the storm stage. Accordingly, bi-conditional Markov chains were established for MSW, translational velocity, and azimuth by the previous stage of these variables and the hurricane stage.

To characterize the hurricane features right after the transition point, we proceeded by statistical analysis on the set of such points (35 transitions in zone H and 60 transitions in zone I) in the "best track" archive (Figure 2). In doing so, we collected storm positions, MSW, translational velocity, and azimuth right before (TS) and after (ET) the transition point (Lat_{TS}, Lon_{TS}, MSW_{TS}, V_{TS}, ϕ_{TS}, Lat_{ET}, Lon_{ET}, MSW_{ET}, V_{ET}, ϕ_{ET}). By transforming these variables into normal distribution and considering their mutual covariance, a multivariate normal distribution was made of them . In our algorithm, whenever the state transitional matrix dictates a transition along the storm track, based on the position and characteristics of the storm in the previous step (the step in which the storm is in a tropical state) the intensity and direction of storm in the next step (the step in which the ensemble is in a extratropical state) were determined followed by the new position of the storm center.

2.3.4 Algorithm flowchart

Figure 3 shows a flowchart for the track generator. The algorithm starts generating ensembles through Monte Carlo simulation. Based on the probability of occurrence, the region in which the storm is generated is randomly selected.

Following the identification of the region in which the storm is formed, its initial position and features are characterised based on random draw from the multivariate distribution of historical genesis points derived from that region. To sample from the multivariate normal distributions, the Gibbs sampler (Geman & Geman, 1984; Gelfand & Smith, 1990) and the algorithm proposed by Li and Ghosh (2015) were used. The taken sample, next, inversely transformed for generation of ensemble genesis. Therefore, at t=0, all the six variables, including the duration of life cycle are initialized. The number of

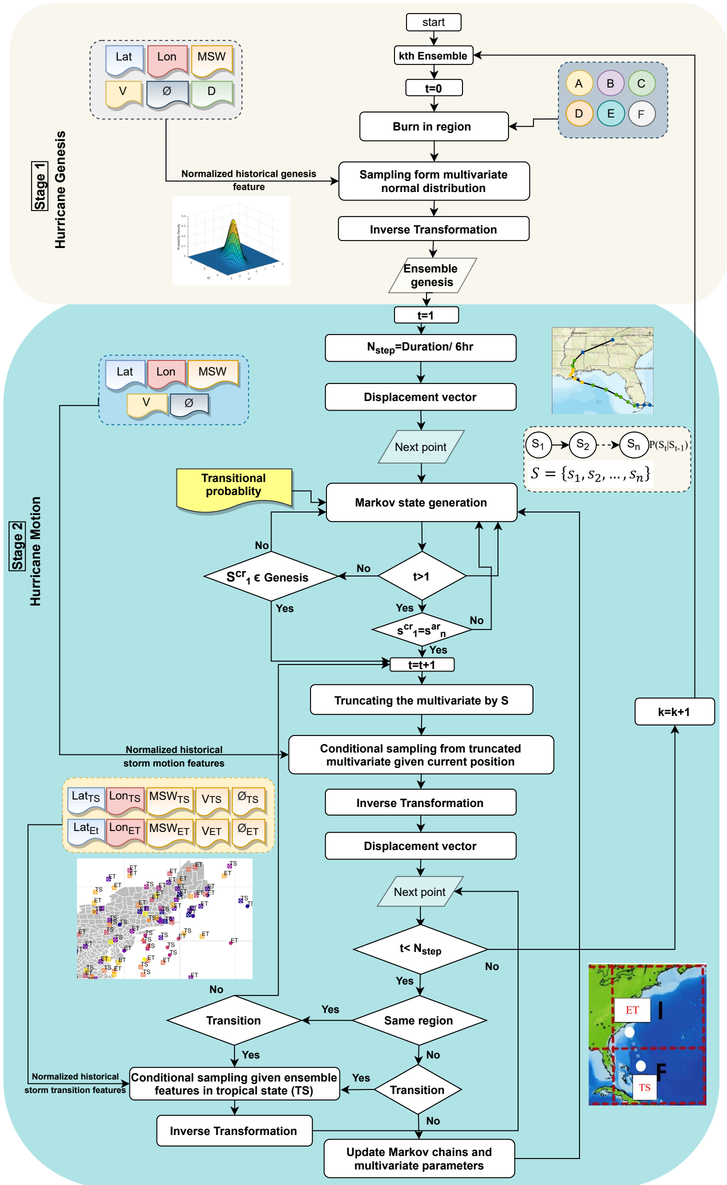

Figure 3. Flowchart for track generator

6-hour time steps the ensemble takes (N_{step}) is obtained by dividing the duration of life cycle by 6 hours. The next position of the ensemble (t=1), then, is determined by the displacement vector obtained from the azimuth and the translational velocity multiplied by time step. Subsequently, the state transition vectors are generated for MSW, translational velocity, and azimuth based on the transitional probabilities of historical storm motion within the same region. At this stage, the only vectors of transition approved are the ones with their first state (s_1) corresponding to the state of the genesis point. The next position of the ensemble, then, is determined by the displacement vector obtained from the azimuth and the translational velocity multiplied by time step. Other characteristics are determined by conditional sampling from the multivariate normal distribution given the state vector of variables and the position of ensemble, and this process is repeated until the ensemble leaves the region of origin. By entering into the neighboring region, the parameters of Markov chains and normal multivariate distributions are updated and the state transition vectors are reconstructed for that region. At this stage, only transition vectors are accepted whose initial state in current region (${s_1}^{cr}$) is in line with the final state of the abandoned region (${s_n}^{ar}$); that is, if an ensemble leaves a region at a speed of 3.5 m/s indicating state 2, the possible realizations of translational velocity needs to start with state 2, for example $\{2,3,3,4,5, \ldots\}$; otherwise, the generated sequence is rejected.

In a similar fashion, the ensemble proceeds in each region based on the updated 6-hour displacement vector and moves into the neighboring regions. Only when the ensemble enters into the regions of H and I (Lat$\geq$ 30°), it may transition to extratropical cyclone. Therefore, in these regions, the trajectory and characteristics of the ensemble may abruptly change due to this transition. After a transition, the next position and characteristics of the ensemble are determined based on conditional sampling from the multivariate normal distribution already made of transition pairs (Figure 2) in best track archive given the position and characteristics of the ensemble in the tropical state. The ensemble, then, continues its course after the turning point. This process is repeated until the termination of life cycle period and then the next ensemble is generated.

To illustrate the capability of our track generator, we evaluated the generated tracks by comparing their statistics with that of historical records on a macro and micro scale. The results of this evaluation are presented in the next section.

3 Results

3.1 Ensemble patch statistics

7174 hurricane ensembles were generated based on the algorithm presented in Figure 1. A comparison between the statistics of the ensemble patch and the observed statistics of historical hurricanes is made in Figure 4.

Figure 4. Histogram and distribution of hurricane explanatory variables for ensembles and "best track" data

Dashed lines in this figure illustrate the average of explanatory variables. The relative error of the mean values (M) and the standard deviation (SD) of these variables is less than 10%. The non-parametric Kolmogorov-Smirnov (K-S) test was applied to test whether the ensemble patch come from the same population as observations. The test statistic (maximum absolute difference between the empirical cumulative probability distribution of ensemble patch and historical records) values of these variables are 0.11, 0.03, 0.04, 0.01, 0.04, and 0.05, respectively. The proximity of the mean values and standard deviation of the ensemble patch and observational data as well as the proximity of the K-S test values to zero indicate that the ensemble patch is a proper representative of the underlying distribution.

The difference in the upper tail of latitude distribution (Figure 4-a) and the higher test statistic are due to the fact that ensembles were not recorded over 46°N degrees latitude as the boundary between the United States and Canada in our algorithm. The two variables whose generation of distribution tails are of high significance for storm hazard assessment are MSW and translational velocity. In the former, the production of the upper tail, i.e. stronger storms, and in the latter, the production of the lower tail, i.e. slow-moving storms, is crucial for hazard assessment. Figure 5 illustrates the quantile-quantile plot of the "best track" data and the ensembles' MSW. According to this figure, the points fall along a line in the middle of the graph and in the extremities, demonstrating the model's set of MSW plausibly come from "best track" data. The same is true for the translational velocity.

Figure 5. "Best track" data and synthetic hurricanes MSW Q-Q plot

In addition to the consistency of the statistics of individual variables to historical records, the compatibility of their mutual correlations for generation of realistic storm paths and hazard is inevitable. Figure 6-a and b reveal that the correlations among the explanatory variables are mutually consistent between the ensemble patch and the "best track" data. The strongest correlation in historical records and ensembles is between latitude and the azimuth of hurricane movement, which is due to the variations of Coriolis force with latitude. Both the ensemble patch and the observations show no correlation between MSW and the longitude of hurricane trajectory. In addition, the correlation between MSW and translational velocity is very insignificant according to "best track" data, which is also apparent in the ensemble patch. Based on the historical records, the mutual correlation of azimuth with MSW and translational velocity is also negligible, which the ensemble patch agrees well with.

Figure 6. mutual correlations between explanatory variables. a) Ensemble patch b) "Best-track" data

3.2 Macro Scale Assessment

When developing TC track ensembles, there is a need to ensure that the proportion of simulated events making landfall in a given area and with a given intensity matches what has been observed or can be extrapolated from historical records. To carry out such an evaluation, a filter was applied to the track generator to select tracks coming within 500 km (typical hurricane size) of an area of interest. Ensembles passing within this specified distance were counted for a given Saffir-Simpson scale and the annual probabilities of occurrence were estimated. Figure 7 provides a comparison between the observed and simulated annual activities of different hurricane categories along the U.S. Atlantic coast.

According to this figure, the ensemble patch, quite similar to historical record, show more intense hurricane activity in the southern United States, including areas located near the North Carolina/South Carolina border, and the central east coast of Florida. Miami observes about 86 hurricanes of category 1 (Figure 7-a), 64 hurricanes of category 2 (Figure 7-c), 43 hurricanes of category 3 (Figure 7-e), 24 hurricanes of category 4 (Figure 7-g), and 5 hurricanes of category 5 (Figure 7-i) per century, (that is, the centers of these hurricanes track through a circle of radius 500 km centered in this location). Correspondingly, 77, 51, 40, 23, and 5 hurricanes hit this area in our statistical model, representing underestimated annual hazard rates for lower categories and a good estimator for the stronger ones.

At the other extreme, New York City has experienced storms of category 1, 2, 3, and 4 with average annual rate of 0.345 (Figure 7-a), 0.110 (Figure 7-c), 0.036 (Figure 7-e), and 0.006 (Figure 7-g), respectively. In addition, category 5 hurricanes have not been reported near this region. Again, the model underestimates the annual occurrence for the weaker storms but provides a good approximation for the stronger ones. Annual rates of 0.097, 0.018, 0.011, 0.005 were observed for the categories of 1 to 4, respectively, through our model. Quite similar to historical records, hurricanes of category 5 fails to be generated in our track generator within this specified radius.

Figure 7. Heat maps for annual probability of Hurricane hits within 500 km. a) Historical recorded category 1. b) Ensemble patch category 1. c) Historical recorded category 2. d) Ensemble patch category 2. e) Historical recorded category 3. f. Ensemble patch category 3. g. historical recorded category 4. h) Ensemble patch category 4. i) Historical recorded category 5. j) Ensemble patch category 5.

The underestimation of annual occurrence for low-category storms is likely due to the application of lag-1 Markovian model, resulting in some of our ensembles getting off the domain before reaching hurricane strength. Examining patterns on partial autocorrelation of MSW time series with 5% significant limits, we observed that 87 out of the total hurricanes have a significant correlation at lag 2 (this number is 41 hurricanes for translational velocity and only 15 hurricanes for azimuth).

3.3 Micro scale assessment

The track generator was tested in micro scale for Miami and New York City, which are completely different in terms of hurricane climatology and frequency. Miami is an example of a city that observes a relatively high incidence of hurricanes per century and many of these storms have not moved into the extratropical stage. Figures 8-a and 8-b show historical tracks and ensembles passing within 100 km of Miami, respectively. There are only 26 tracks passing within 100 km of Miami during the period in question including hurricanes King (1950), Cleo (1964), David (1979), Andrew (1992), Ivan (2004), Katrina (2005), Floyd (1999), Gordon (2000), and Irene (2011), versus 1311 storms out of 7177 storms that were statistically generated in our model (Figure 8-b). For comparison with "best track" data, the hurricane types and position of storm centers around Miami are illustrated in Figure 9.

Figure 8. Hurricanes passing within 100 km of Miami. a) "Best track" data. b) Synthetic tracks

Figure 9-a shows that about 70% of historical storms moved into this area with the strength of a hurricane. This area has experienced hurricane categories of 1 to 4. Similarly, this number slightly increases to 75%, 9-b, which represents a high agreement with the existing records. In addition to generation of history of potential storms, our model shows that storms with hurricane category of 5 are also likely to pass within this specified distance (Figure9-b) with a probability of only 1.5%.

Figure 9. Hurricane position and category within 100 km of Miami. a) "Best track" data. b) Synthetic tracks

Unlike Miami which has a relatively rich record of storms, and most of which have not undergone strong interactions with extratropical systems, New York City has only had a handful of storms in its history, and many of those have been affected by interactions with extratropical systems. In this case, historical records are not sufficient to reasonably estimate storm hazard, however, due to the occurrence of rare but very destructive storms in this area, hurricane hazard assessment is still of interest. Hurricane positions and categories within 100 kilometers of New York City are shown in Figure 10-a. The most extreme of these storms are hurricanes Able (1952), Diane (1955), Donna (1960), Agnes (1972), Belle (1976), Bertha (1996), Floyd (1999), Gordon (2000), and Irene (2011). Figure 10-b illustrates the patch of ensemble within this specified region. According to this figure, 225 of the 7177 ensembles generated move into this area, which has experienced a limited number of storms in the past.

Figure 10. Hurricanes passing within 100 km of New York City. a) "Best track" data. b) Synthetic tracks

According to Figure 11-a, the strongest hurricane this city has observed within the radius of 100 km, is hurricane of category 2. Only about 20 percent of the historical storms entered into this area with hurricane strength. Similarly, in Figure 11-b, a low proportion of ensembles have entered this area with hurricane strength. According to this figure, the model was well able to generate storms with the history of categories observed in this area. A hurricane of category 3 is also formed in the offshore of this region, showing the capability of the model in generating extremely low probable but intensive hazards.

Figure 11. Hurricane position and category within 100 km of New York City. a) "Best track" data. b) Synthetic tracks

We excluded hurricane Sandy from the "best track" data and rebuilt our model by re-estimating the parameters of Markov chains and multivariate distributions to illustrate the capability of our model for reconstruction of unique trajectories.

Unlike most hurricanes on a northward track along the US coast curve east and out to sea before they reach New York, Sandy took unusual path, turned sharply west and came at a perpendicular angle to the coast of New York City. It was this shift that helped push the storms massive surge directly at the south-facing parts of the city. Similarly, while most of our ensemble members are well out to sea, a small number of ensembles bend toward the west. Out of 7177 ensembles, we found only two tracks that, had a similar track to Sandy,, moving westward and landfalling near New York City. Figure 12 shows these two tracks alongside Sandy trajectory.

Figure 12. Sandy-like cyclone trajectories

According to this figure, our algorithm prevents the two ensembles from moving out to sea, creating a curved trajectory with a turning between 35°N and 40°N latitude. Ensemble No. 979, similar to Sandy, approaches the shore as a category 1 hurricane . Ensemble No. 3264, although similar to Sandy, shifted westward and made landfall near New York City, did not reach hurricane strength. The behavior of any of the ensembles after transitioning, although different from Hurricane Sandy, is not inconsistent with historical observations. Historical records indicate that the behavior of storms after reaching a transition is very uncertain and chaotic and storms may transition into a stronger storm or higher category (hurricane Sandy), weaker storm or lower category (ensemble No. 979), and remains in the same state or category (ensemble No. 3264).

Both of our Sandy-like trajectories show smaller displacements before their turning point, which is a pattern commonly observed in North Atlantic tropical cyclone paths. In other words, the trajectory points of the storm's path before turning westward, are more tightly spaced, fitting the trend observed by our model.

As mentioned earlier, hurricane hazard is driven by multiple factors rather than a single one. In addition to wind intensity, which has been the cornerstone of hurricane risk and damage models in most previous studies, translational velocity is an important agent in determining the severity of hurricane hazard in coastal areas and presenting even a greater influence than the wind intensity. Here, to demonstrate the capability of our model to reasonably make synthetic storms, the distribution of these two variables within 100 km distance from New York City and Miami is illustrated as a box plot in Figures 13-a and 13-b, respectively.

Figure 13. Box plot of MSW and translational velocity within 100 km of Miami and New York City

The lower, upper, and middle quartiles of MSW generated within 100 km of New York City and Miami are slightly less than the corresponding quartiles of "best track" data at this distance, indicating the presence of bias in the model, which could be due to the use of lag-1 Markov chain. However, the model produces a history of local potential wind speed. The upper, middle, and lower quartiles of "best track" data are 40, 52.5, and 60 knots for New York City, and 70, 85, 110 knots for Miami. The corresponding quartiles for the model are: 35, 45, 50 knots for New York City, and 55, 75, and 95 for Miami. The maximum difference in quartiles belongs to the upper and lower quartiles of Miami, which are equal to 15 knots.

According to Figure 13-b, the upper, middle, and lower quartiles of historical records for translational velocity are 6.3, 10.1, and 12.4 m/s for New York City, and 4.7, 5.4, 6.2 m/s knots for Miami, respectively. The corresponding quartiles for the model are: 5.5, 9.2, 12.5 m/s for New York City, and 3.0, 4.4, and 6.1 m/s for Miami, sequentially. Similar to MSW, where model quartiles are slightly lower than historical records, the quartiles of translational speed are lower than the corresponding values of historical hurricanes in the regions of interest, which again reveals a bias in the model.

Contrary to the MSW, where the upper tail increases hazard intensity, slower moving storms have proven to result in higher risks when reaching the coast (Gomes et al., 2015). According to this figure, our track generator demonstrates its capability to synthesize slow-moving storms such as those normally observed in these regions. Both historical record and the model show slower-moving storms with stronger wind surrounding the area of Miami than New York City, causing more intense episodes of inundation and destruction in Miami.

Computing the K-S test statistic in two dimensional space implies that the MSW-translational speed sets of ensemble patch are drawn from the same underlying joint distribution as historical records. The values of K-S test statistic are 0.23 and 0.31 for Miami and New York City, respectively, which are lower than their corresponding critical values of 0.25, and 0.32.

4 Conclusion

Frequency analysis on local storm intensities is not capable of storm hazard assessment for areas such as New York City, that have experienced only a limited number of severe storms in history, due to insufficient observations. Ensemble generation is critical for circumventing this difficulty, taken into account in this study. The soundness of our algorithm for generating hurricane ensembles was evaluated by statistical comparison with historical record. Such a comparison joined by K-S test suggests that the statistics of generated ensembles are generally in good agreement with the observed statistics of the historical record.

In macro scale test of our algorithm, the hurricane activity of ensemble patch within 500 km radius of US counties conforms broadly to the trend of historical record, suggesting the proposed algorithm is a viable approach for hurricane hazard assessment. In micro scale our algorithm was tested on Miami and New York City with quite different hurricane climatology. The results illustrate the capability of our model in generating countless severe storms in data-sparse regions. Our track generator produces a history of local potential maximum sustained wind and translational speed from the underlying distribution in these two regions. This is important because storms with similar intensity and different translational speeds have different effects in one area; that is, a large category 2 hurricane may cause a greater hazard than category 4.

Our results also show that unique trajectories similar to Hurricane Sandy can be statistically reconstructed even by excluding their trajectory from historical records. Among the ensembles generated, two tracks were found that followed the unique trajectory of Hurricane Sandy after crossing the latitude of 30°N, curved sharply west rather than east and out to sea.

The outlined methodology in this paper can be used for hurricane hazard assessments and risk modeling in hurricane-prone regions. We recommend interested researchers in the area of Tc risk assessment to either (i) re-generate storm events with high potential of occurrence in areas with both high and low hurricane frequencies; or (ii) to use such dataset to compare the statistics of surge ensembles with an observed record of a near gauge to see weather the record is a good representative of storm surge hazard in the region. We plan to do this in future work.

Acknowledgments

The author would like to appreciate Ravi Varadhan, Alan Genz et al, Ting Fung et al, Giorgio Alfredo Spedicato, Ryan Andrew Peterson, and Robert J. Hijmans for their valuable "condMVNorm", "mvtnorm", "tmvmixnorm", "markovchain", "bestNormalize", "geosphere" R packages, respectively. All data used in this research is publicly available at NOAA'a best-track archives.

References

Bloemendaal, N., Haigh, I. D., de Moel, H., Muis, S., Haarsma, R. J., & Aerts, J. C. (2020). Generation of a global synthetic tropical cyclone hazard dataset using storm. *Scientific Data*, *7*(1), 1–12.

Burroughs, W. J. (2007). *Climate change: a multidisciplinary approach.* Cambridge University Press.

Coles, S., & Simiu, E. (2003). Estimating uncertainty in the extreme value analysis of data generated by a hurricane simulation model. *Journal of engineering mechanics*, *129*(11), 1288–1294.

Done, J. M., Bruyère, C. L., Ge, M., & Jaye, A. (2014). Internal variability of north atlantic tropical cyclones. *Journal of Geophysical Research: Atmospheres*, *119*(11), 6506–6519.

Edmund, H., Chamberlain, S., & Ram, K. (2014). rnoaa: Noaa climate data from r. [Computer software manual]. Retrieved from `https://github.com/ropensci/`

rnoaa (R package version 0.1.9.99)

Emanuel, K. (2005). Increasing destructiveness of tropical cyclones over the past 30 years. *Nature*, *436*(7051), 686–688.

Emanuel, K., Ravela, S., Vivant, E., & Risi, C. (2006). A statistical deterministic approach to hurricane risk assessment. *Bulletin of the American Meteorological Society*, *87*(3), 299–314.

Freeman, A. C., & Ashley, W. S. (2017). Changes in the us hurricane disaster landscape: the relationship between risk and exposure. *Natural hazards*, *88*(2), 659–682.

Garner, A. J., Mann, M. E., Emanuel, K. A., Kopp, R. E., Lin, N., Alley, R. B., ... Pollard, D. (2017). Impact of climate change on new york citys coastal flood hazard: Increasing flood heights from the preindustrial to 2300 ce. *Proceedings of the National Academy of Sciences*, *114*(45), 11861–11866.

Gelfand, A. E., & Smith, A. F. (1990). Sampling-based approaches to calculating marginal densities. *Journal of the American statistical association*, *85*(410), 398–409.

Geman, S., & Geman, D. (1984). Stochastic relaxation, gibbs distributions, and the bayesian restoration of images. *IEEE Transactions on pattern analysis and machine intelligence*(6), 721–741.

Gneiting, T., & Raftery, A. E. (2005). Weather forecasting with ensemble methods. *Science*, *310*(5746), 248–249.

Gomes, M. P., Pinho, J. L., do Carmo, J. S. A., & Santos, L. (2015). Hazard assessment of storm events for the battery, new york. *Ocean & Coastal Management*, *118*, 22–31.

Hallegatte, S., Hourcade, J.-C., & Dumas, P. (2007). Why economic dynamics matter in assessing climate change damages: illustration on extreme events. *Ecological economics*, *62*(2), 330–340.

Hoque, M. A.-A., Phinn, S., Roelfsema, C., & Childs, I. (2016). Assessing tropical cyclone impacts using object-based moderate spatial resolution image analysis: a case study in bangladesh. *International Journal of Remote Sensing*, *37*(22), 5320–5343.

Lai, Y., Li, J., Gu, X., Chen, Y. D., Kong, D., Gan, T. Y., ... Wu, G. (2020). Greater flood risks in response to slowdown of tropical cyclones over the coast of china. *Proceedings of the National Academy of Sciences*, *117*(26), 14751–14755.

Lam, J. S. L., Liu, C., & Gou, X. (2017). Cyclone risk mapping for critical coastal infrastructure: Cases of east asian seaports. *Ocean & Coastal Management*, *141*, 43–54.

Li, Y., & Ghosh, S. K. (2015). Efficient sampling methods for truncated multivariate normal and student-t distributions subject to linear inequality constraints. *Journal of Statistical Theory and Practice*, *9*(4), 712–732.

Lin, N., Emanuel, K., Oppenheimer, M., & Vanmarcke, E. (2012). Physically based assessment of hurricane surge threat under climate change. *Nature Climate Change*, *2*(6), 462–467.

Lin, N., Kopp, R. E., Horton, B. P., & Donnelly, J. P. (2016). Hurricane sandys flood frequency increasing from year 1800 to 2100. *Proceedings of the National Academy of Sciences*, *113*(43), 12071–12075.

Loridan, T., Khare, S., Scherer, E., Dixon, M., & Bellone, E. (2015). Parametric modeling of transitioning cyclone wind fields for risk assessment studies in the western north pacific. *Journal of Applied Meteorology and Climatology*, *54*(3), 624–642.

Mei, W., Kamae, Y., Xie, S.-P., & Yoshida, K. (2019). Variability and predictability of north atlantic hurricane frequency in a large ensemble of high-resolution atmospheric simulations. *Journal of Climate*, *32*(11), 3153–3167.

Mohleji, S., & Pielke Jr, R. (2014). Reconciliation of trends in global and regional economic losses from weather events: 1980–2008. *Natural Hazards Review*, *15*(4), 04014009.

Pielke Jr, R. A., Gratz, J., Landsea, C. W., Collins, D., Saunders, M. A., & Musulin, R. (2008). Normalized hurricane damage in the united states: 1900–2005. *Natural Hazards Review*, *9*(1), 29–42.

Puotinen, M. (2007). Modelling the risk of cyclone wave damage to coral reefs using gis: a case study of the great barrier reef, 1969–2003. *International Journal of Geographical Information Science*, *21*(1), 97–120.

Reed, A. J., Mann, M. E., Emanuel, K. A., Lin, N., Horton, B. P., Kemp, A. C., & Donnelly, J. P. (2015). Increased threat of tropical cyclones and coastal flooding to new york city during the anthropogenic era. *Proceedings of the National Academy of Sciences*, *112*(41), 12610–12615.

Shuckburgh, E., Mitchell, D., & Stott, P. (2017). Hurricanes harvey, irma and maria: how natural were thesenatural disasters'? *Wthr*, *72*(11), 353–354.

Taylor, H. T., Ward, B., Willis, M., & Zaleski, W. (2010). The saffir-simpson hurricane wind scale. *Atmospheric Administration: Washington, DC, USA*.

Varlas, G., Katsafados, P., Papadopoulos, A., & Korres, G. (2018). Implementation of a two-way coupled atmosphere-ocean wave modeling system for assessing air-sea interaction over the mediterranean sea. *Atmospheric Research*, *208*, 201–217.

Vickery, P. J. (2005). Simple empirical models for estimating the increase in the central pressure of tropical cyclones after landfall along the coastline of the united states. *Journal of applied meteorology*, *44*(12), 1807–1826.

Villarini, G., Luitel, B., Vecchi, G. A., & Ghosh, J. (2019). Multi-model ensemble forecasting of north atlantic tropical cyclone activity. *Climate Dynamics*, *53*(12), 7461–7477.

Weinkle, J., Landsea, C., Collins, D., Musulin, R., Crompton, R. P., Klotzbach, P. J., & Pielke, R. (2018). Normalized hurricane damage in the continental united states 1900–2017. *Nature Sustainability*, *1*(12), 808–813.

Woodruff, J. D., Irish, J. L., & Camargo, S. J. (2013). Coastal flooding by tropical cyclones and sea-level rise. *Nature*, *504*(7478), 44–52.

Wooten, R. D., & Tsokos, C. P. (2008). A markovian analysis of hurricane transitions. *Neural, Parallel and Scientific Computations*, *16*(1), 1.

Workgroup, N. L. S. (2015). Guidance for considering the use of living shorelines. *Silver Spring, Maryland: National Oceanic and Atmospheric Administration, 36p*.

Yonekura, E., & Hall, T. M. (2011). A statistical model of tropical cyclone tracks in the western north pacific with enso-dependent cyclogenesis. *Journal of Applied Meteorology and Climatology*, *50*(8), 1725–1739.

Figure 1.

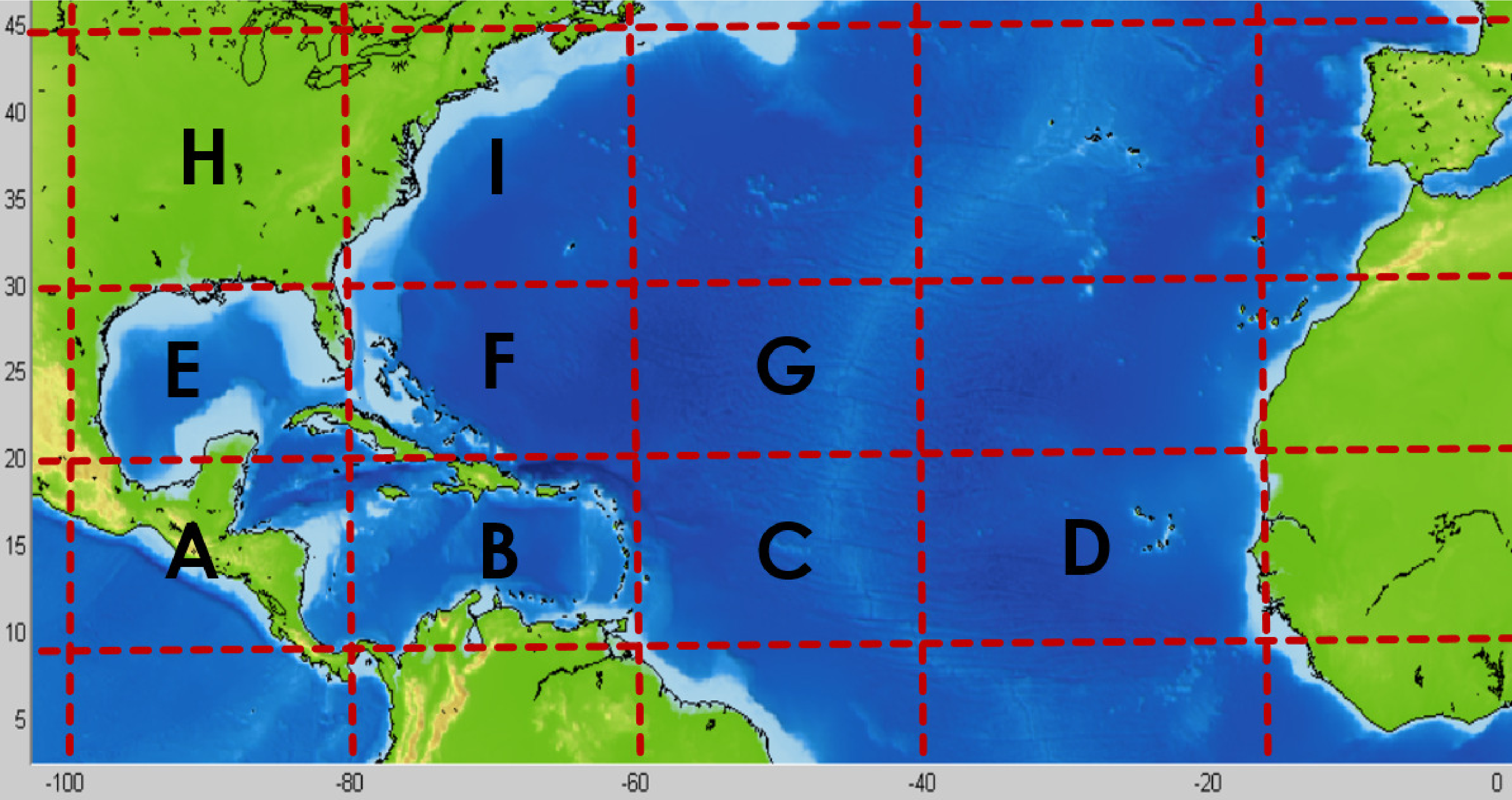

H
I
E
F
G
A
B
C
D
45
40
35
30
25
20
15
10
5
-100
-80
-60
-40
-20
0

Figure 2.

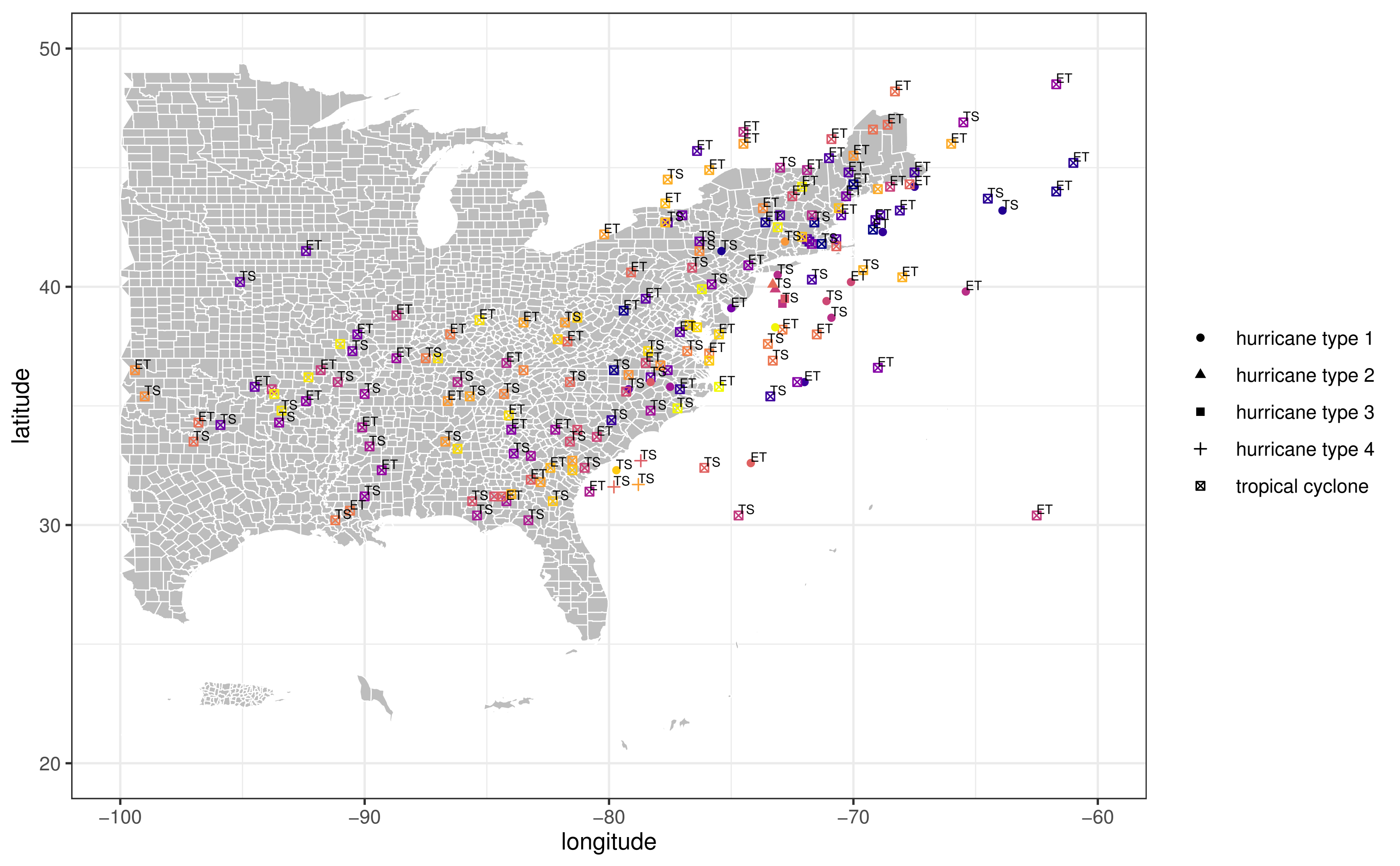

50
40
30
20
latitude
−100
−90
−80
−70
−60
longitude
hurricane type 1
hurricane type 2
hurricane type 3
hurricane type 4
tropical cyclone

Figure 3.

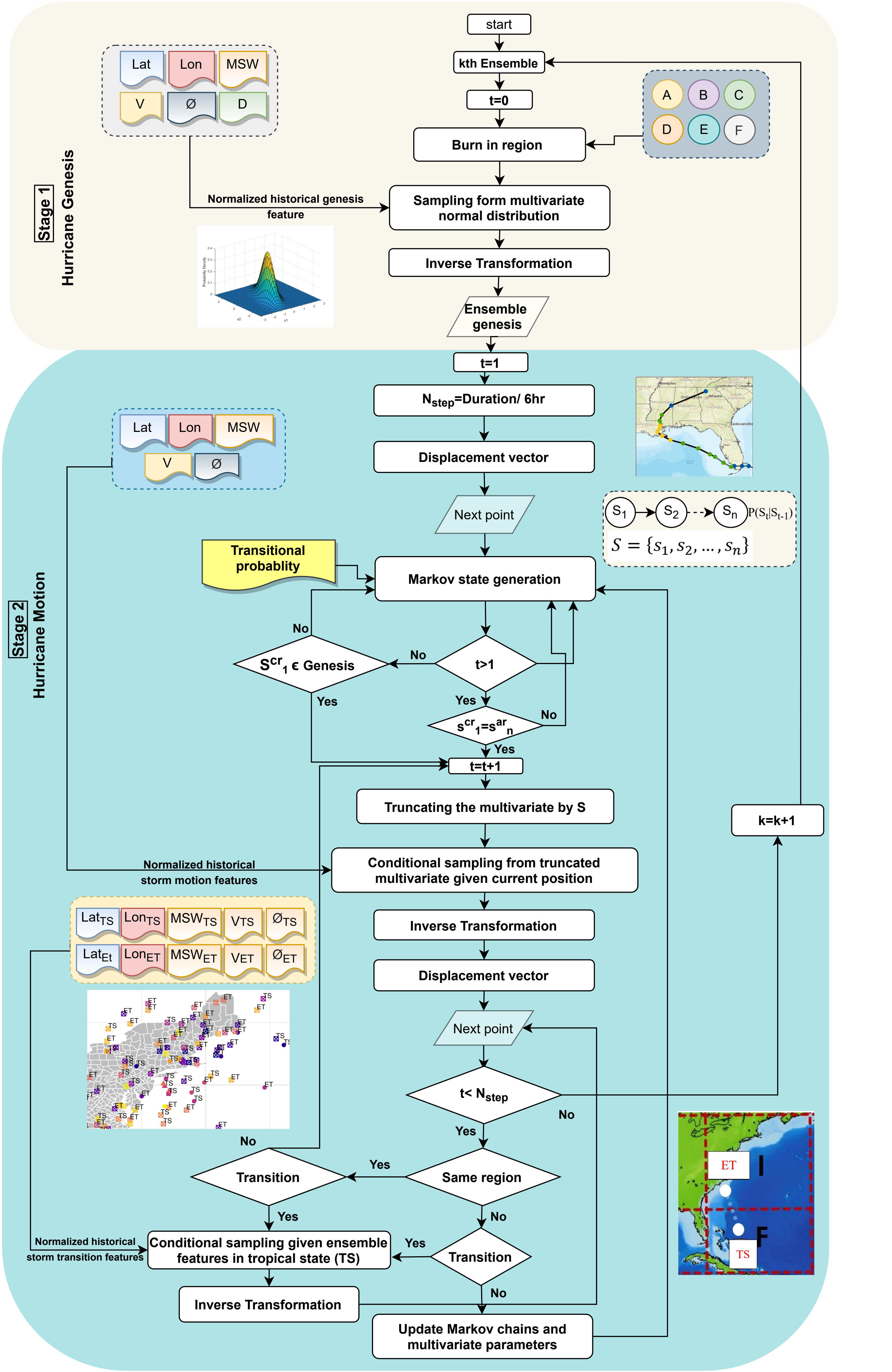

Stage 1
Hurricane Genesis
start
kth Ensemble
t=0
Lat
Lon
MSW
V
Ø
D
A
B
C
D
E
F
Burn in region
Normalized historical genesis feature
Sampling form multivariate normal distribution
Inverse Transformation
Ensemble genesis
Stage 2
Hurricane Motion
t=1
N_step=Duration/ 6hr
Displacement vector
Next point
Lat
Lon
MSW
V
Ø
S_1
S_2
S_n
P(S_t|S_t-1)
S = {s_1, s_2, ..., s_n}
Transitional probablity
Markov state generation
No
S^cr_1 ϵ Genesis
No
t>1
Yes
Yes
No
s^cr_1=s^ar_n
Yes
t=t+1
Truncating the multivariate by S
k=k+1
Normalized historical storm motion features
Conditional sampling from truncated multivariate given current position
Lat_TS
Lon_TS
MSW_TS
V_TS
Ø_TS
Lat_Et
Lon_ET
MSW_ET
V_ET
Ø_ET
Inverse Transformation
Displacement vector
Next point
t< N_step
No
Yes
No
Transition
Yes
Same region
ET
TS
Yes
No
Normalized historical storm transition features
Conditional sampling given ensemble features in tropical state (TS)
Yes
Transition
No
Inverse Transformation
Update Markov chains and multivariate parameters

Figure 4-1.

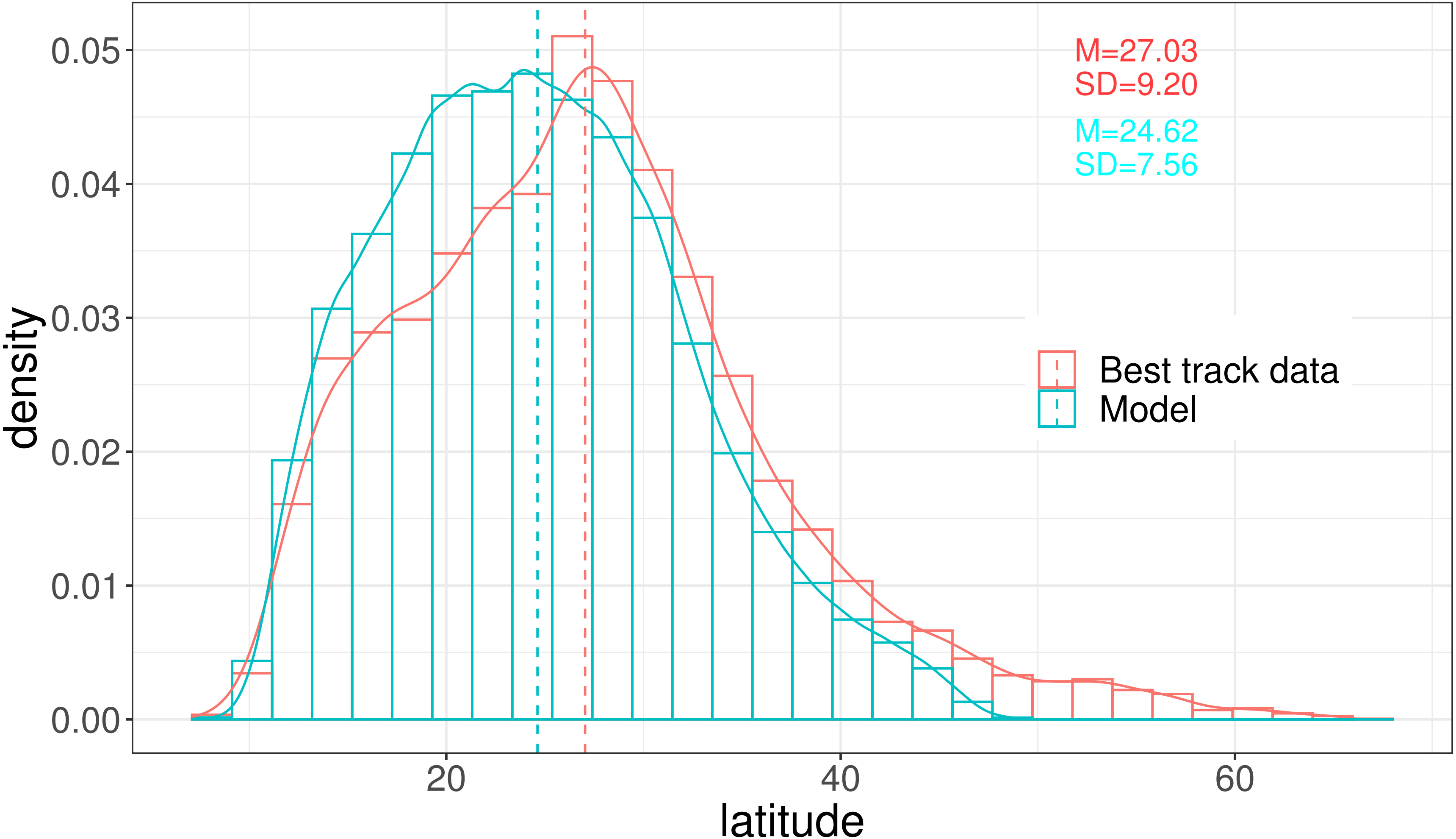
M=27.03
SD=9.20
M=24.62
SD=7.56
Best track data
Model
density
latitude
0.00
0.01
0.02
0.03
0.04
0.05
20
40
60
(a)

Figure 4-2.

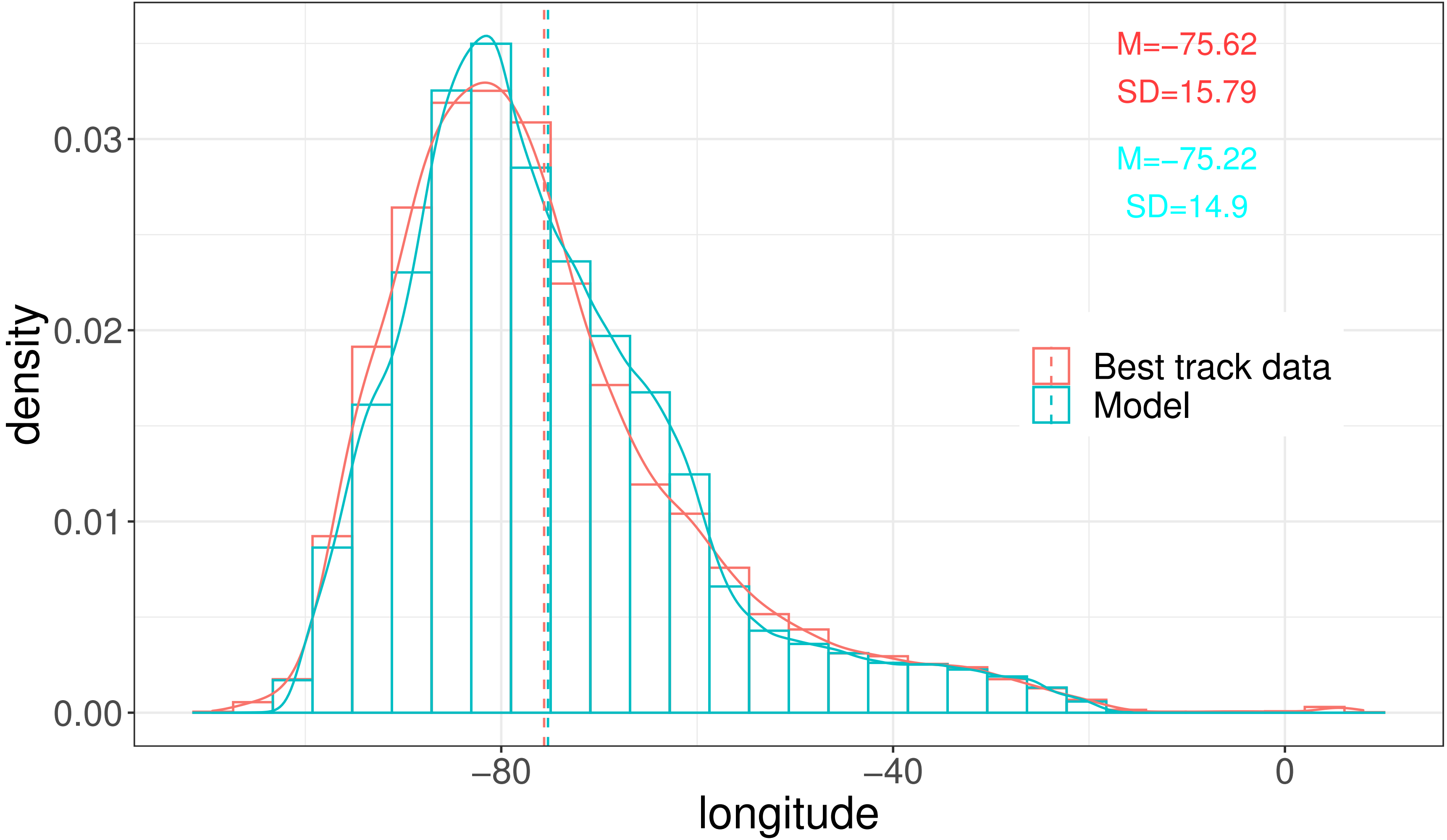

M=−75.62
SD=15.79
M=−75.22
SD=14.9
Best track data
Model
density
0.00
0.01
0.02
0.03
longitude
−80
−40
0

(b)

Figure 4-3.

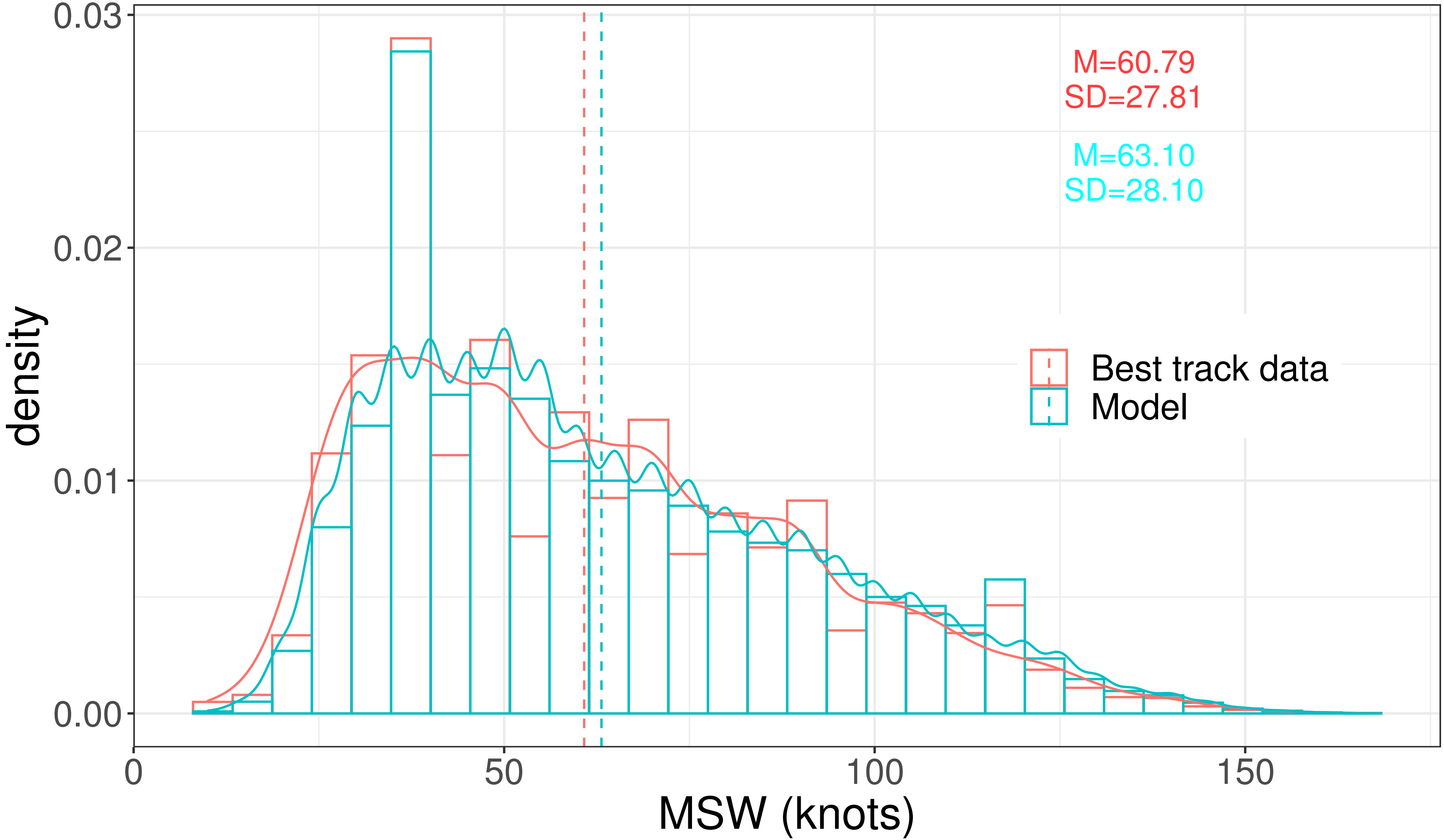

M=60.79
SD=27.81
M=63.10
SD=28.10
Best track data
Model
density
0.03
0.02
0.01
0.00
0
50
100
150
MSW (knots)

(c)

Figure 4-4.

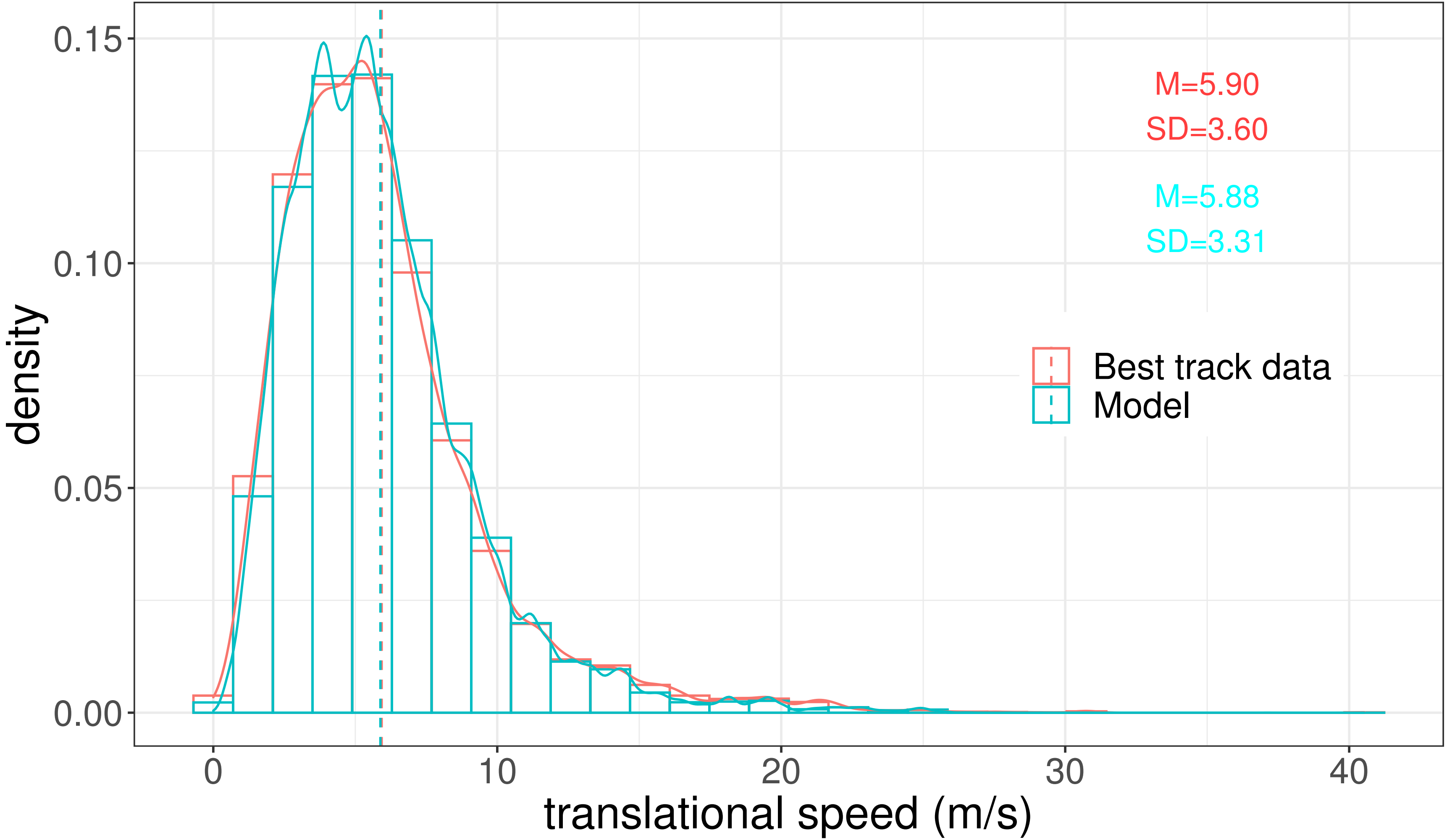

M=5.90
SD=3.60
M=5.88
SD=3.31
Best track data
Model
density
translational speed (m/s)
0.15
0.10
0.05
0.00
0
10
20
30
40

(d)

Figure 4-5.

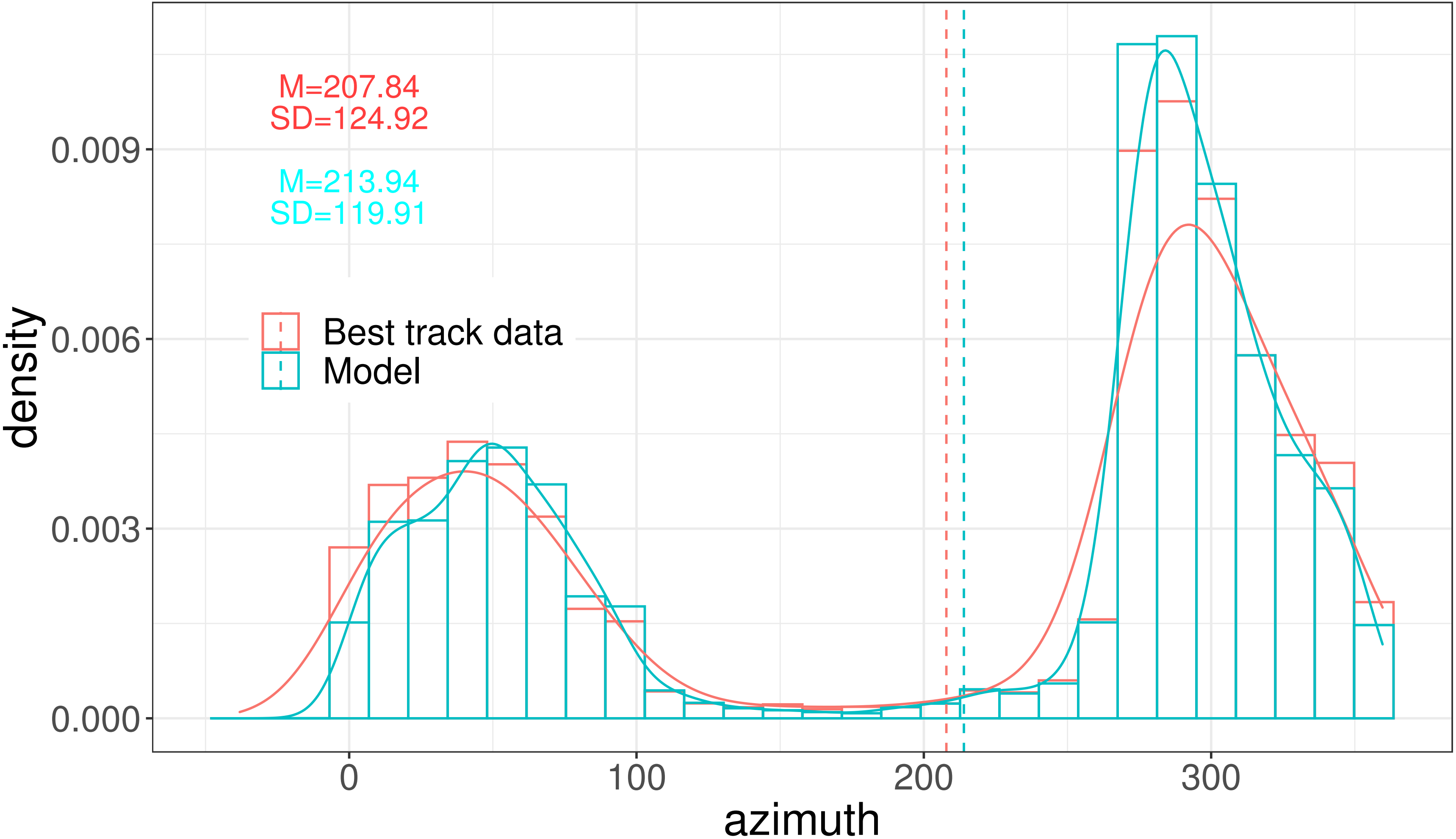
M=207.84
SD=124.92
M=213.94
SD=119.91
Best track data
Model
density
0.009
0.006
0.003
0.000
0
100
200
300
azimuth
(e)

Figure 4-6.

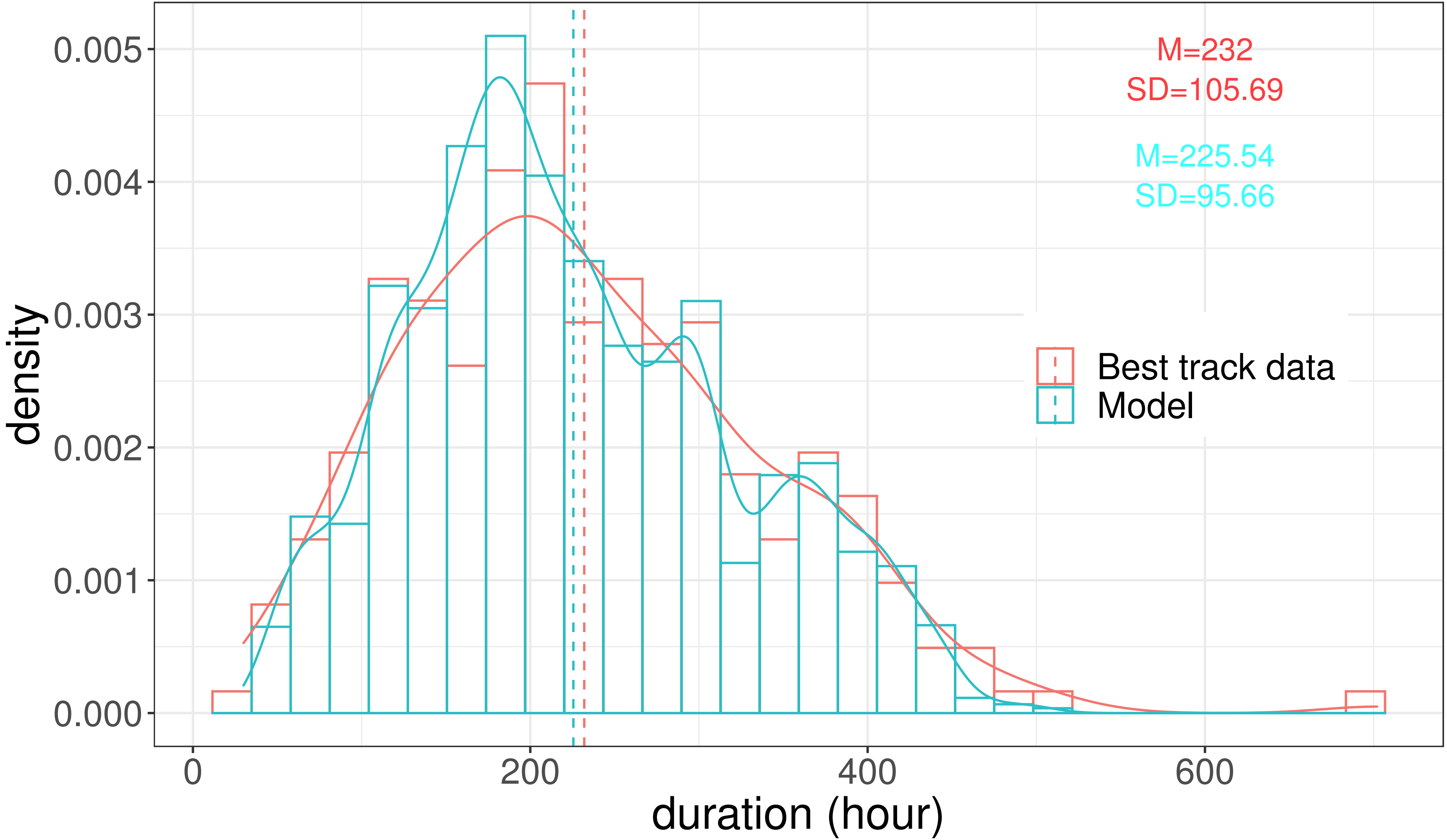
M=232
SD=105.69
M=225.54
SD=95.66
Best track data
Model
density
0.005
0.004
0.003
0.002
0.001
0.000
0
200
400
600
duration (hour)

(f)

Figure 5.

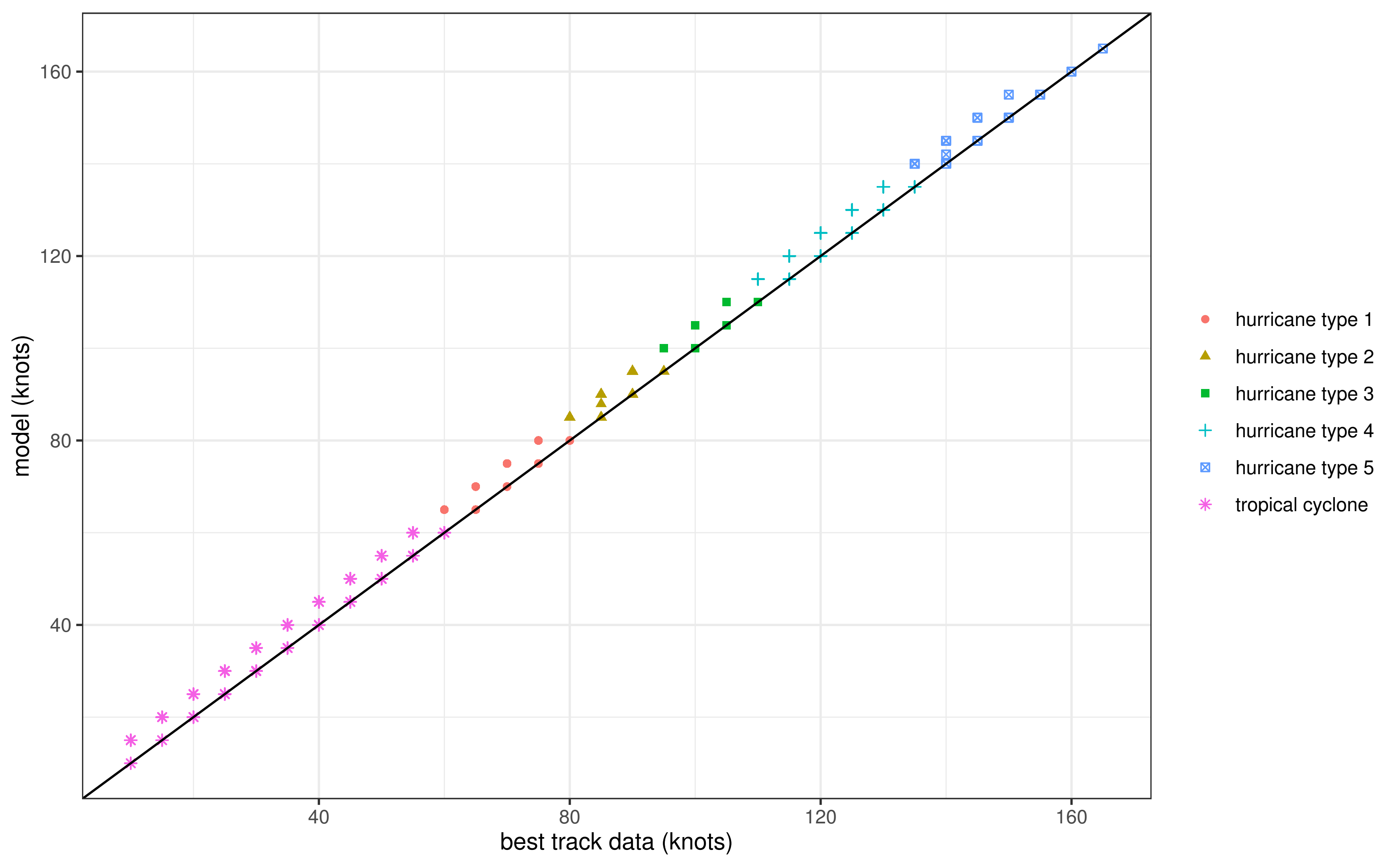
model (knots)
best track data (knots)
40
80
120
160
40
80
120
160
hurricane type 1
hurricane type 2
hurricane type 3
hurricane type 4
hurricane type 5
tropical cyclone

Figure 6.

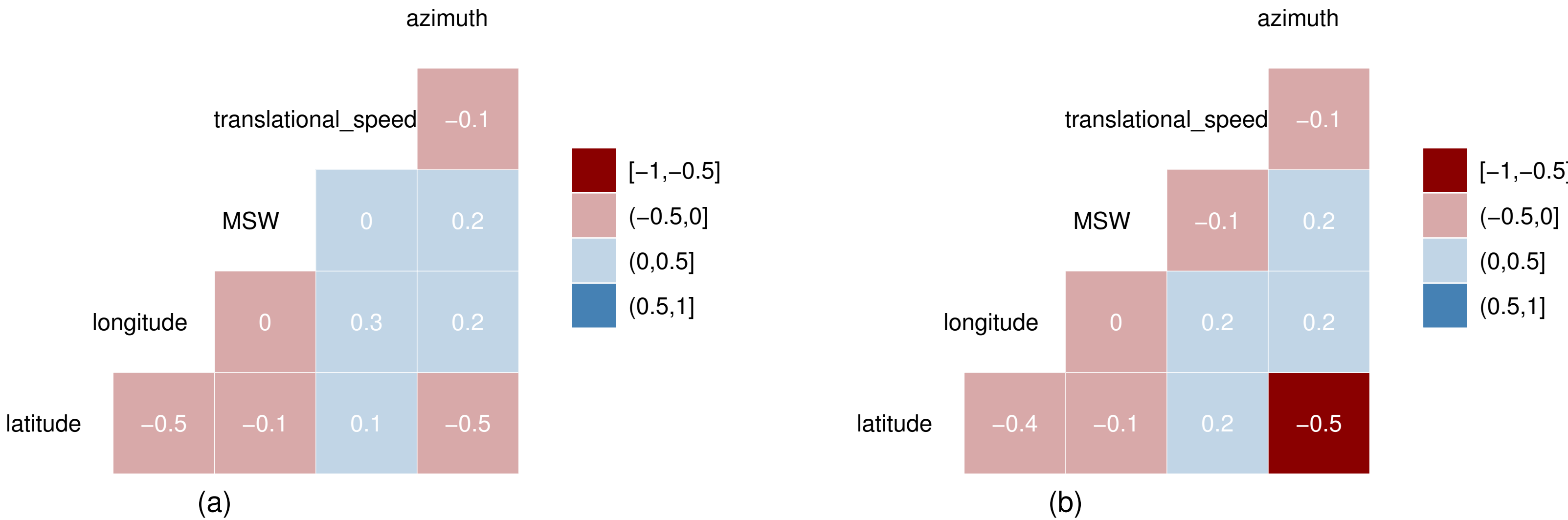

azimuth
translational_speed
MSW
longitude
latitude
–0.1
0
0.2
0
0.3
0.2
–0.5
–0.1
0.1
–0.5
[–1,–0.5]
(–0.5,0]
(0,0.5]
(0.5,1]
(a)
azimuth
translational_speed
MSW
longitude
latitude
–0.1
–0.1
0.2
0
0.2
0.2
–0.4
–0.1
0.2
–0.5
[–1,–0.5]
(–0.5,0]
(0,0.5]
(0.5,1]
(b)

Figure 7-1.

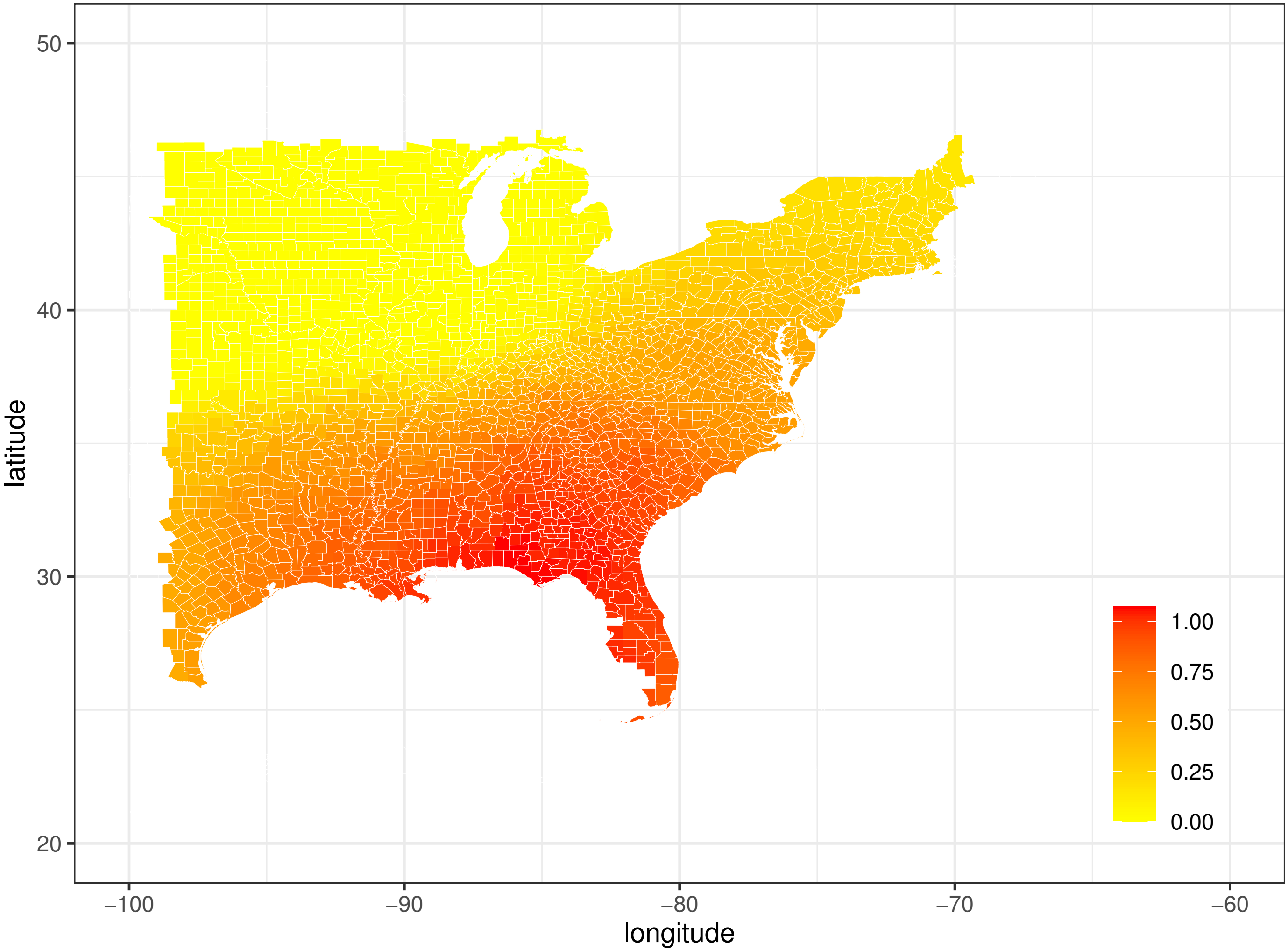
50
40
30
20
latitude
−100
−90
−80
−70
−60
longitude
1.00
0.75
0.50
0.25
0.00
(a)

Figure 7-2.

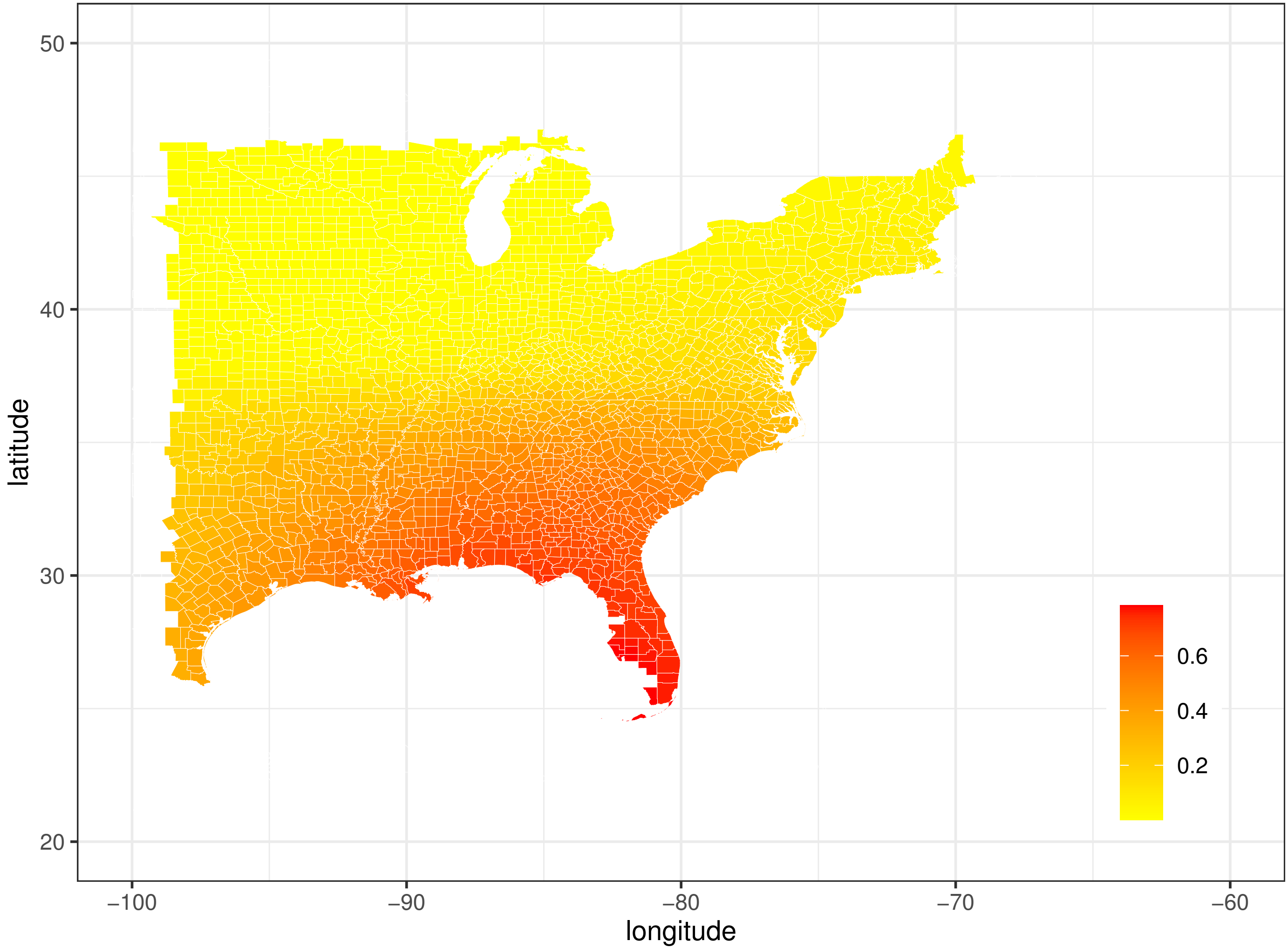

(b)

Figure 7-3.

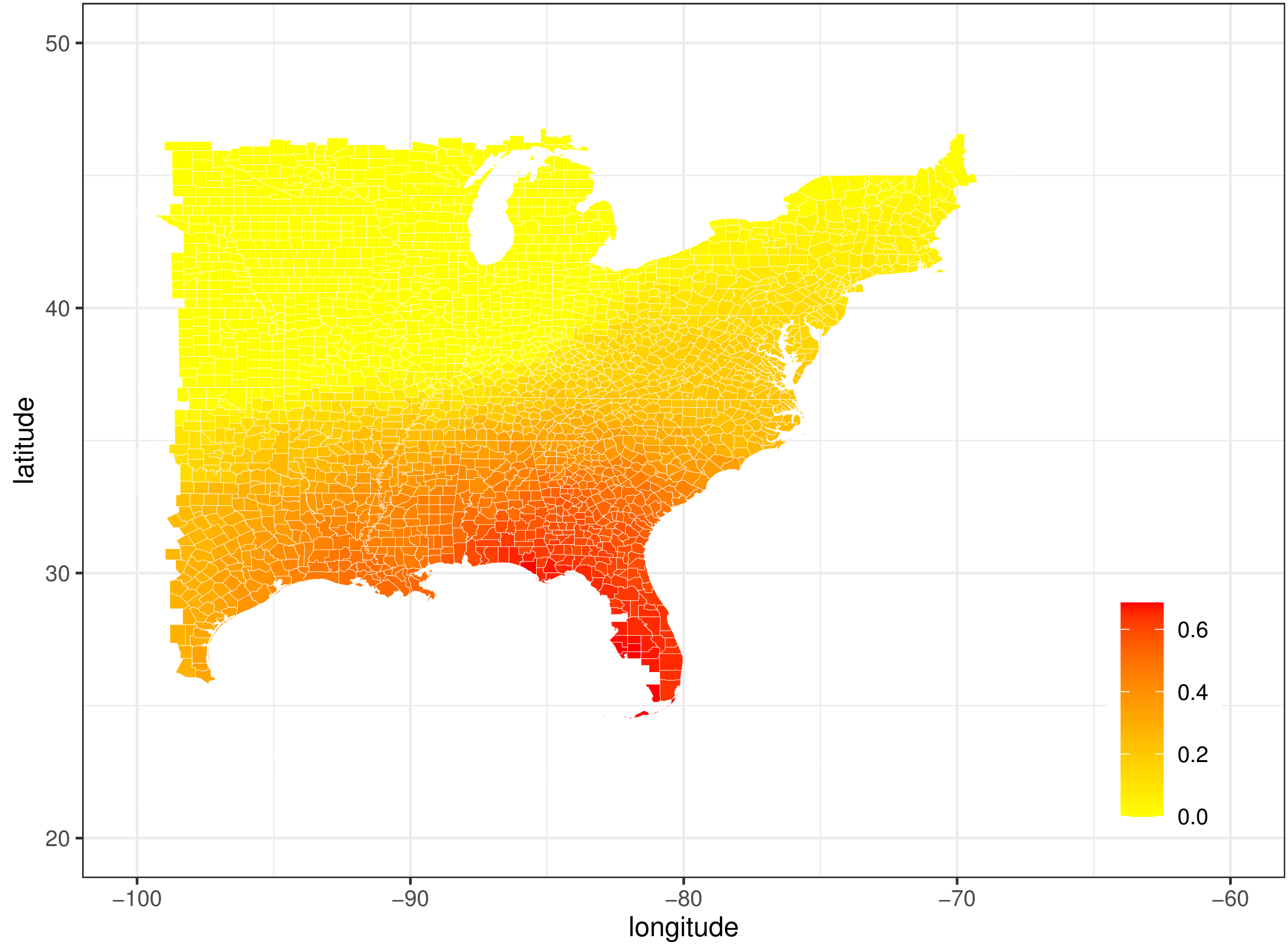

(c)

Figure 7-4.

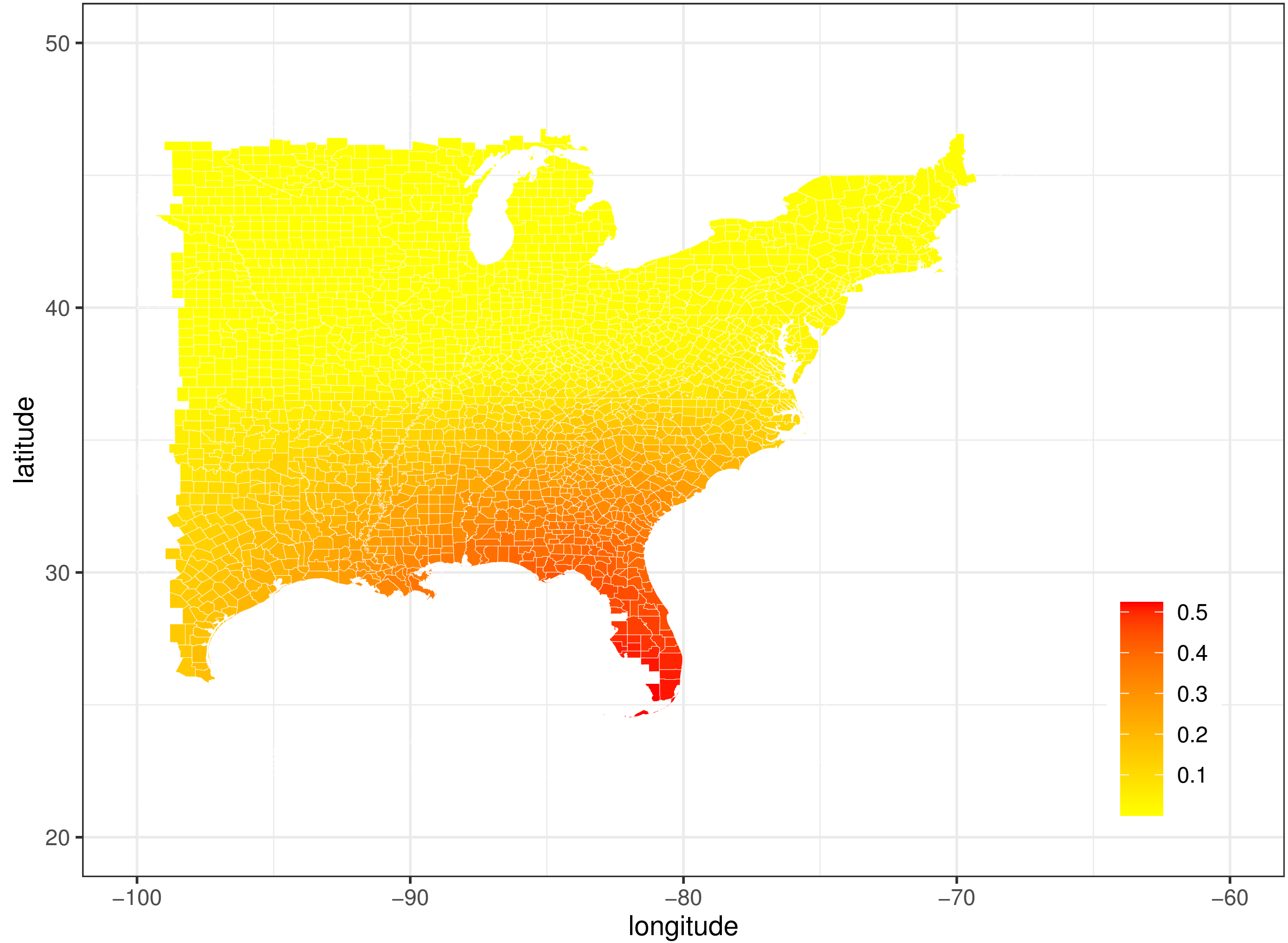

(d)

Figure 7-5.

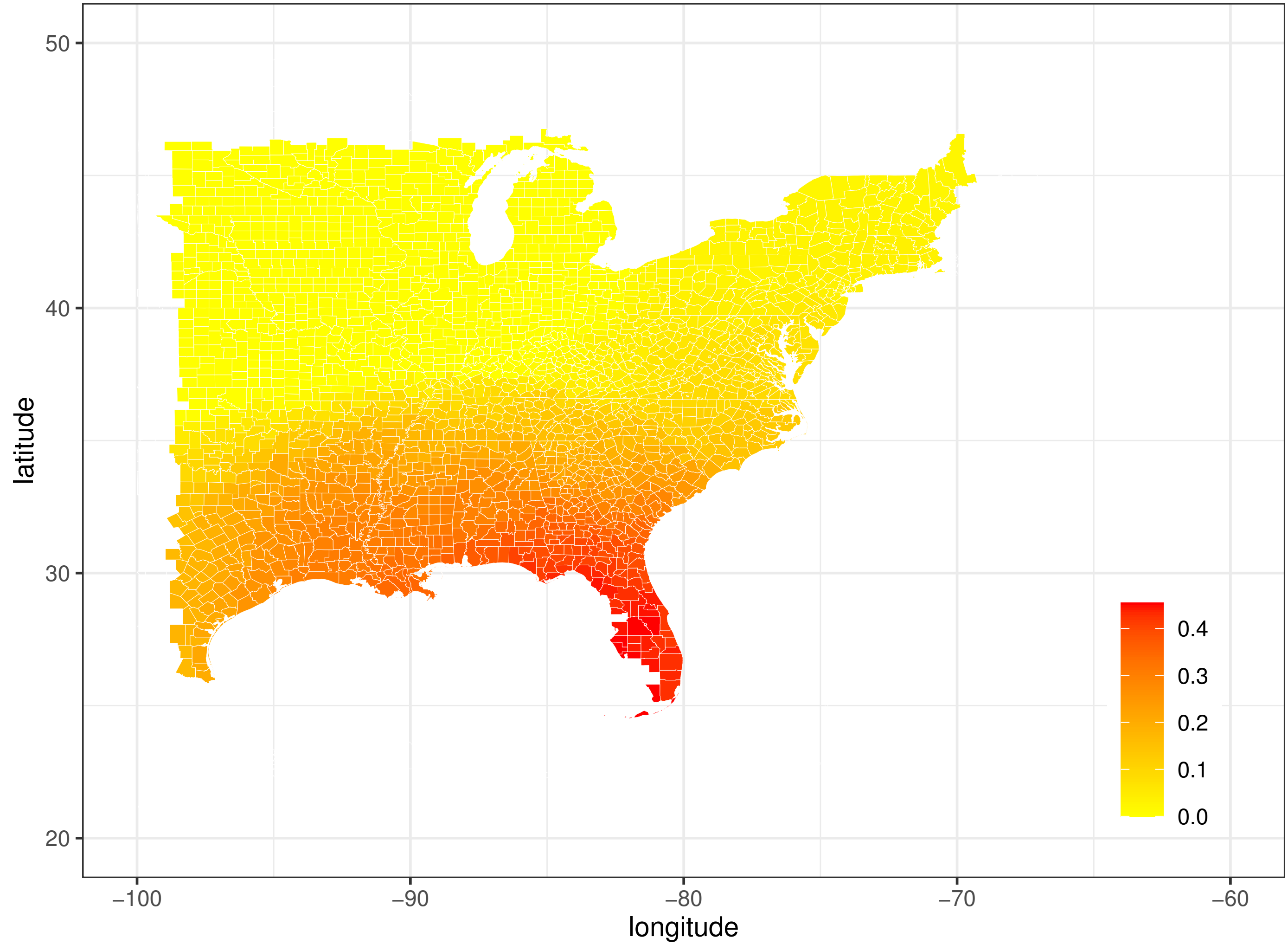

(e)

Figure 7-6.

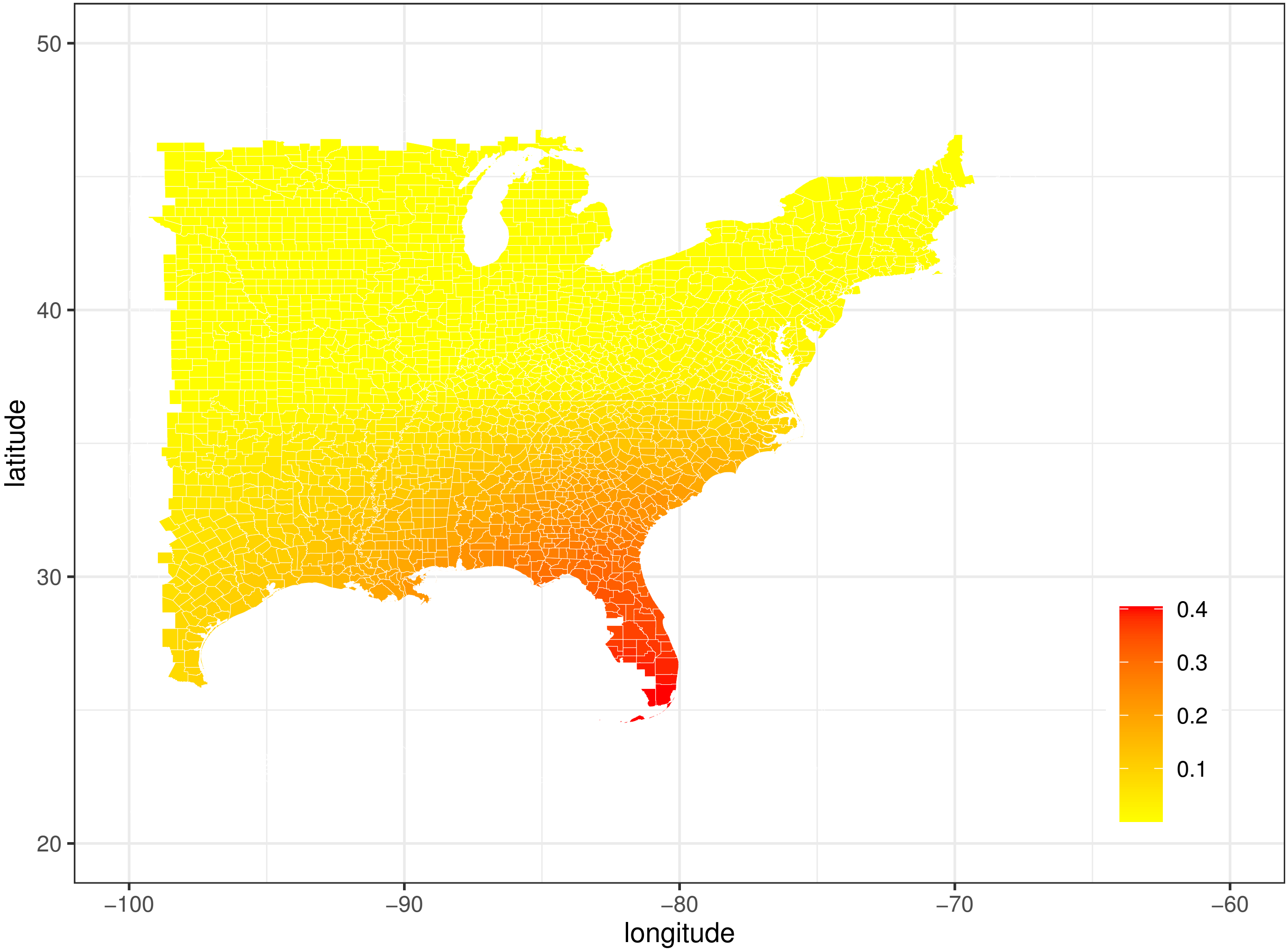

(f)

Figure 7-7.

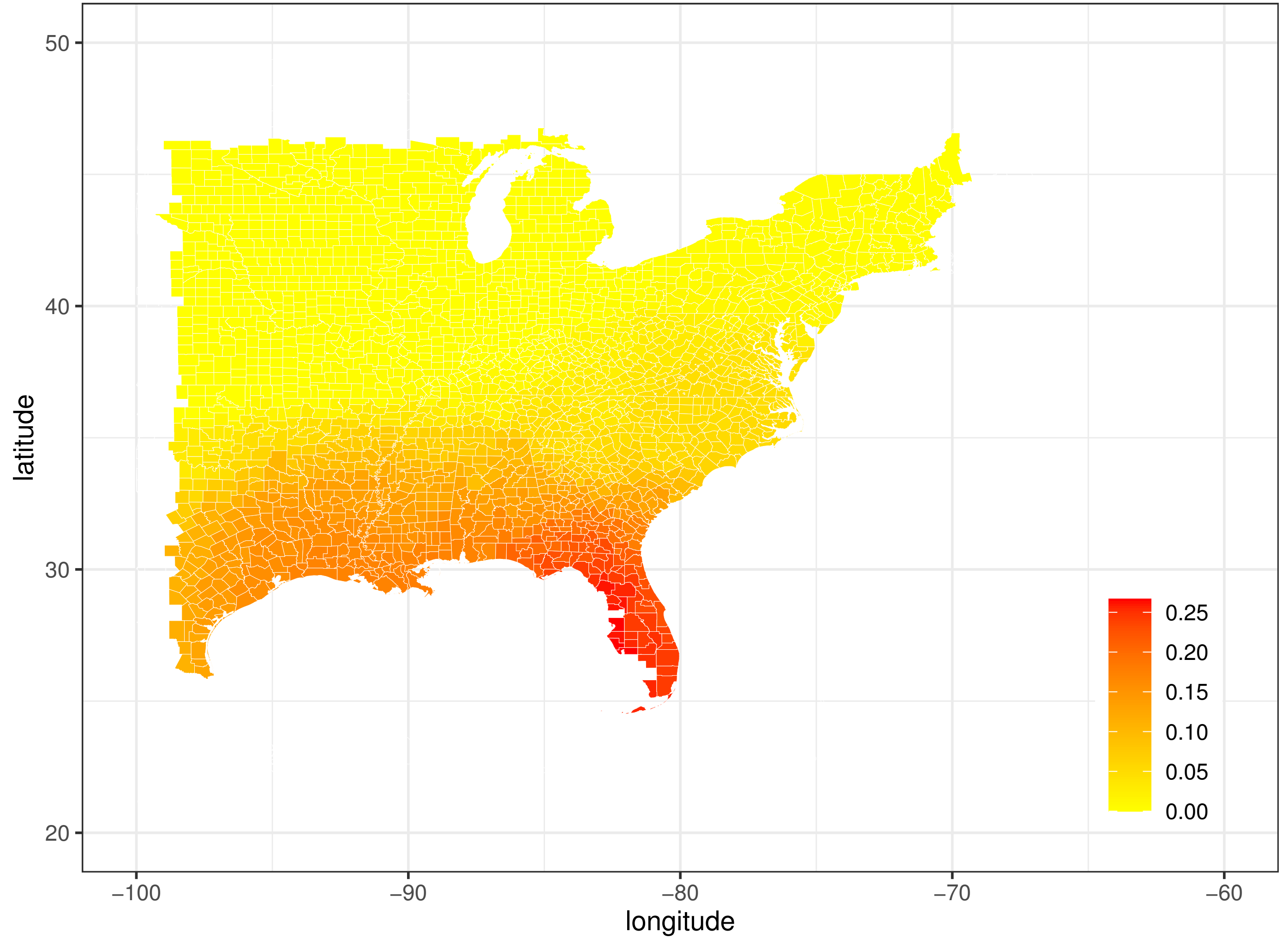
50
40
30
20
latitude
−100
−90
−80
−70
−60
longitude
0.25
0.20
0.15
0.10
0.05
0.00

(g)

Figure 7-8.

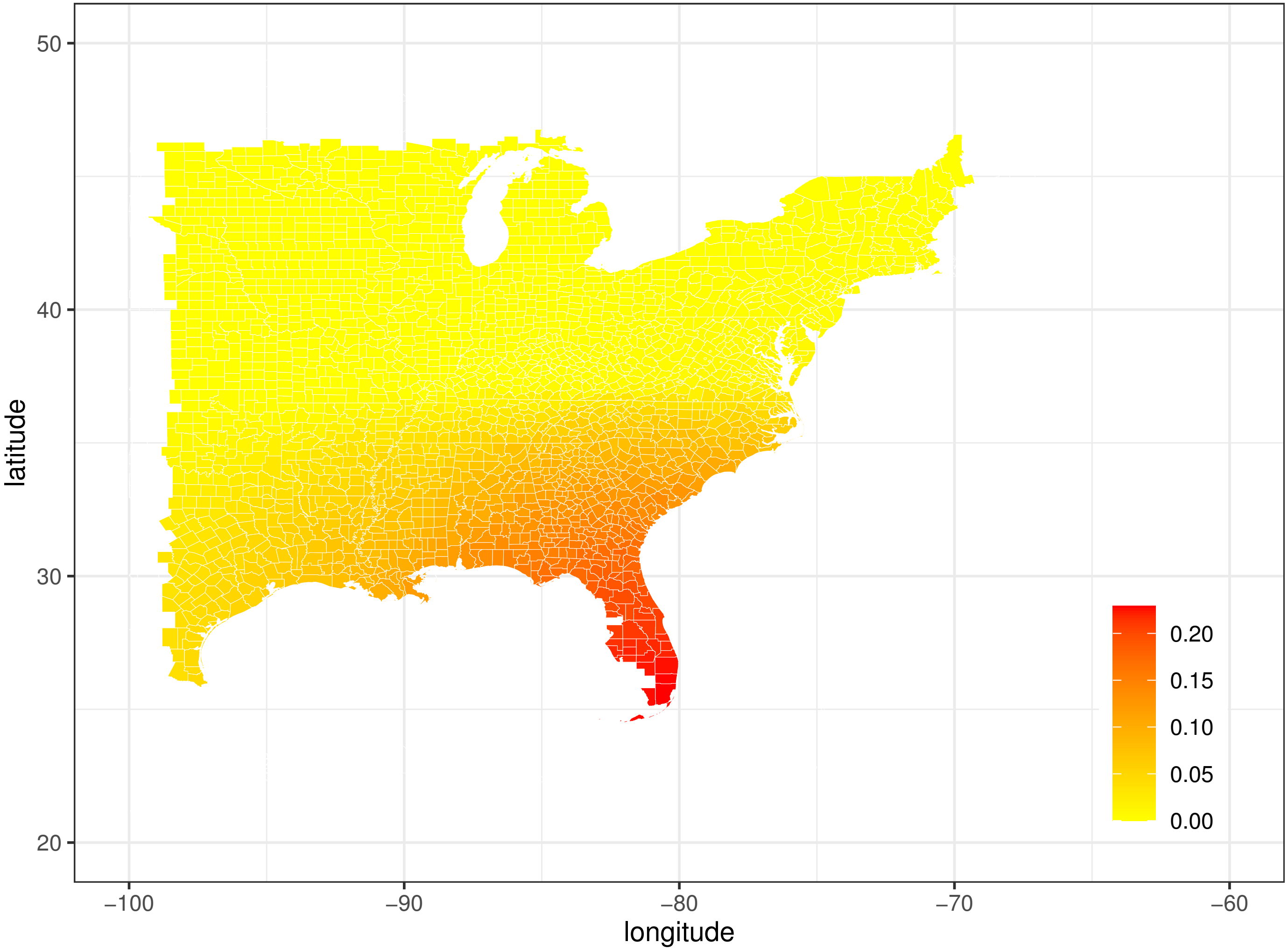

50
40
30
20
latitude
−100
−90
−80
−70
−60
longitude
0.20
0.15
0.10
0.05
0.00

(h)

Figure 7-9.

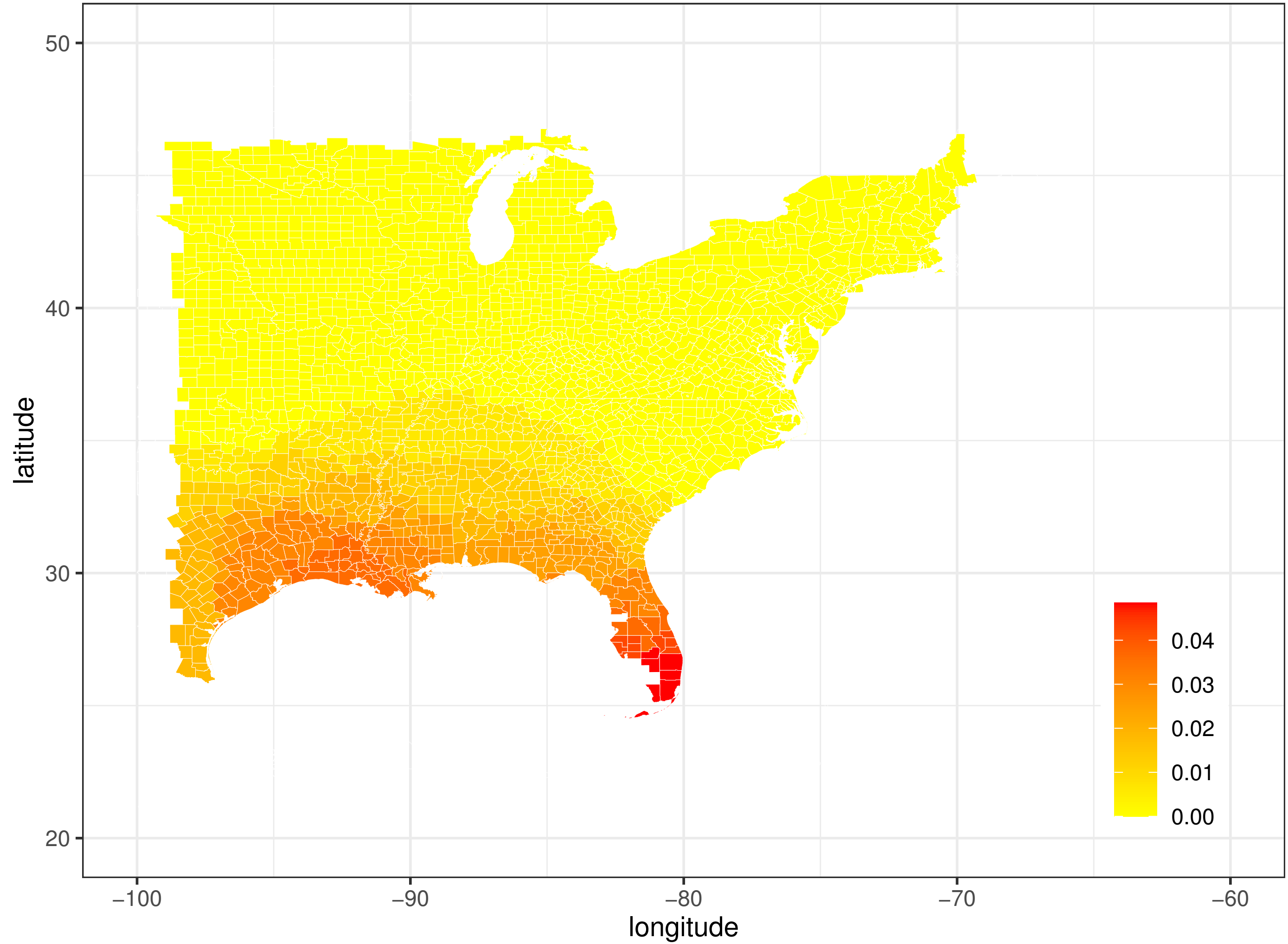
50
40
30
20
latitude
−100
−90
−80
−70
−60
longitude
0.04
0.03
0.02
0.01
0.00

(i)

Figure 7-10.

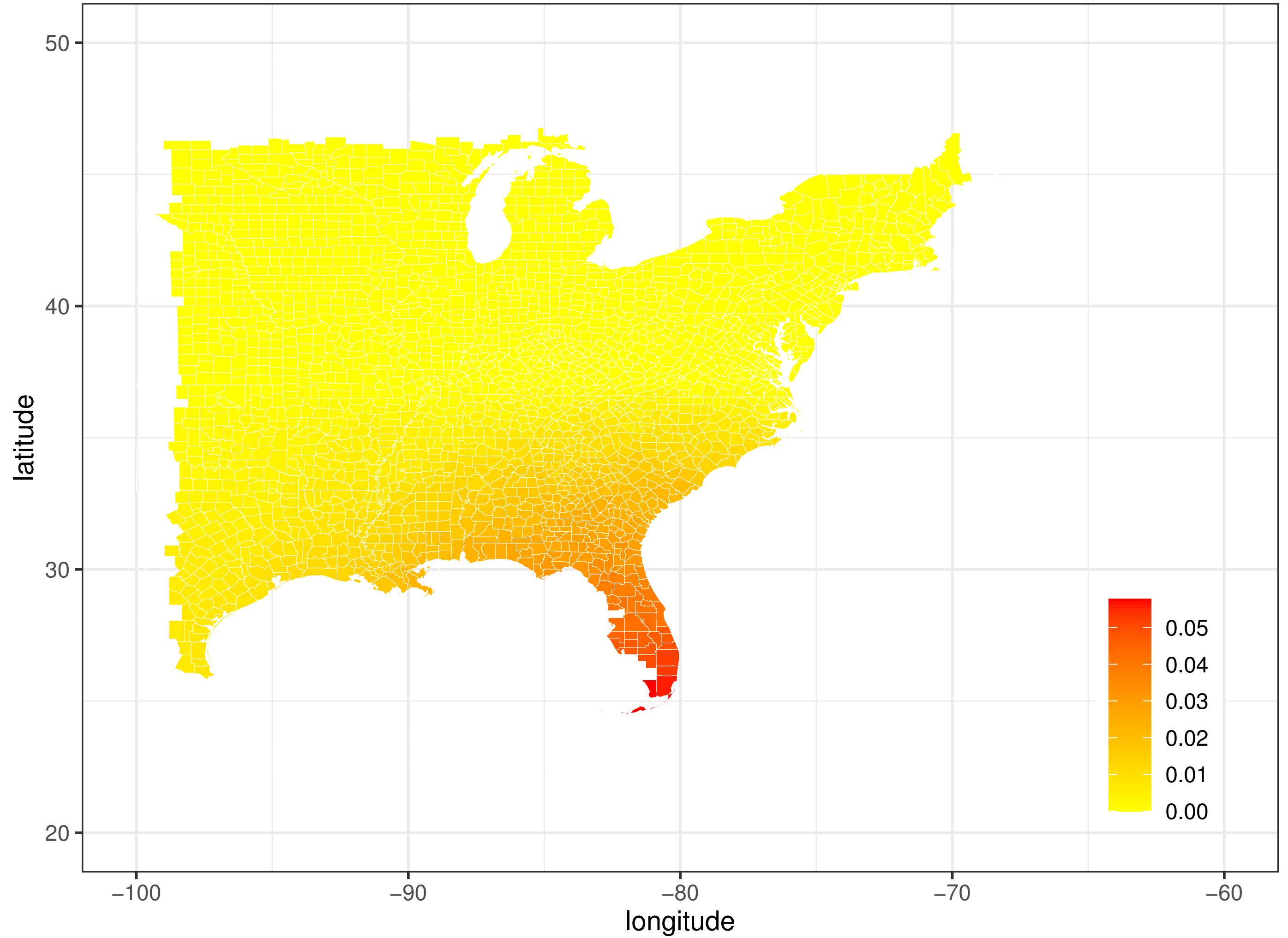
50
40
30
20
latitude
−100
−90
−80
−70
−60
longitude
0.05
0.04
0.03
0.02
0.01
0.00

(j)

Figure 8.

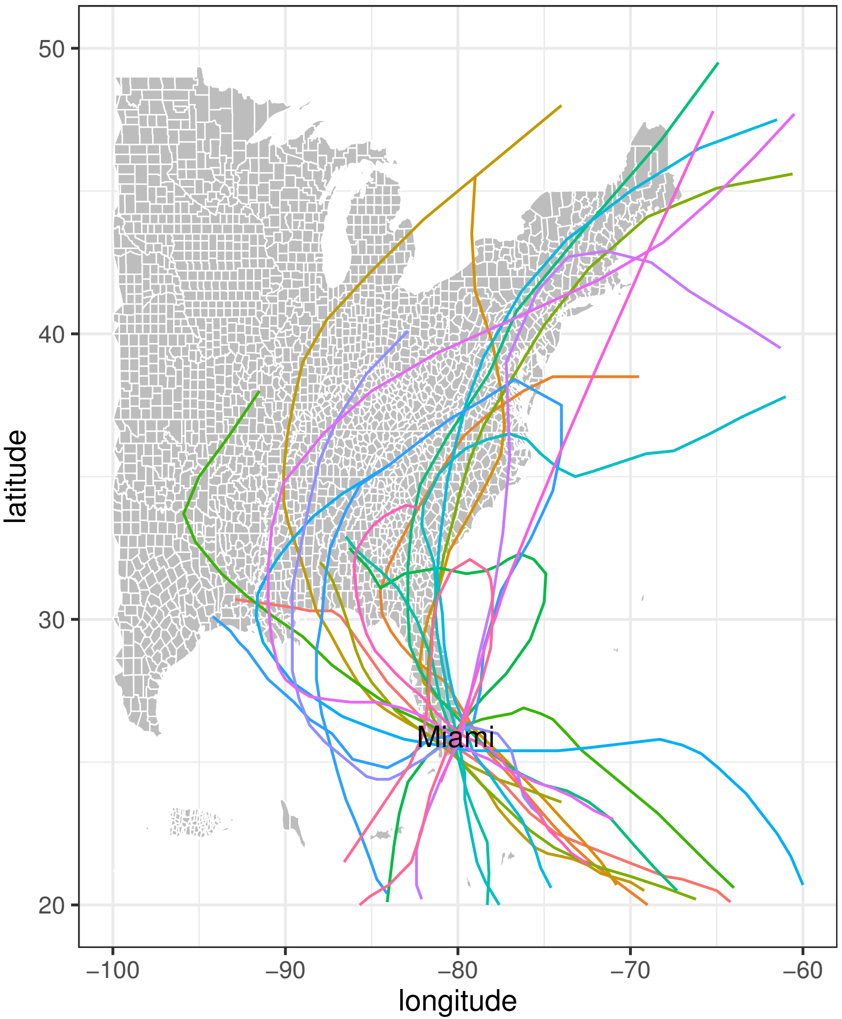
50
40
30
20
−100
−90
−80
−70
−60
latitude
longitude
Miami

(a)

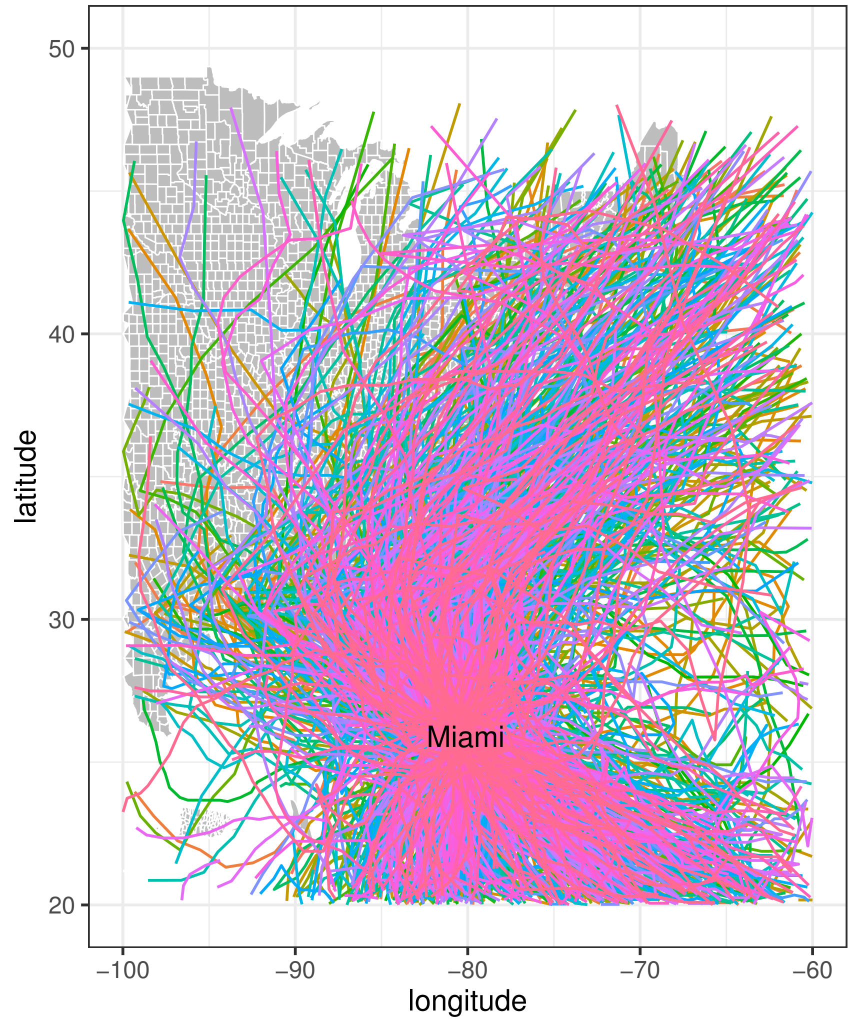
50
40
30
20
−100
−90
−80
−70
−60
latitude
longitude
Miami

(b)

Figure 9.

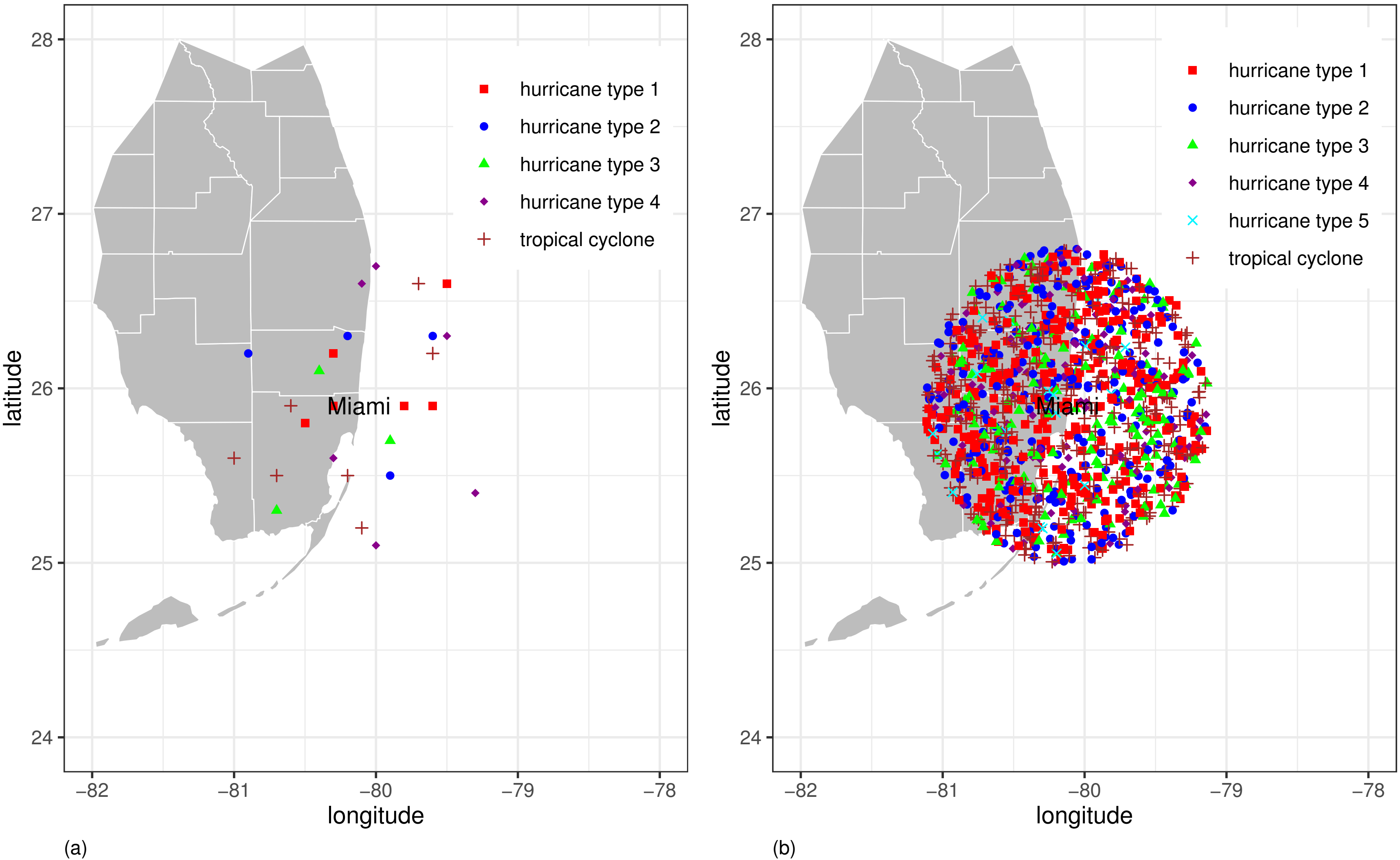

28
27
26
25
24
latitude
−82
−81
−80
−79
−78
longitude
Miami
hurricane type 1
hurricane type 2
hurricane type 3
hurricane type 4
hurricane type 5
tropical cyclone
(a)
(b)

Figure 10.

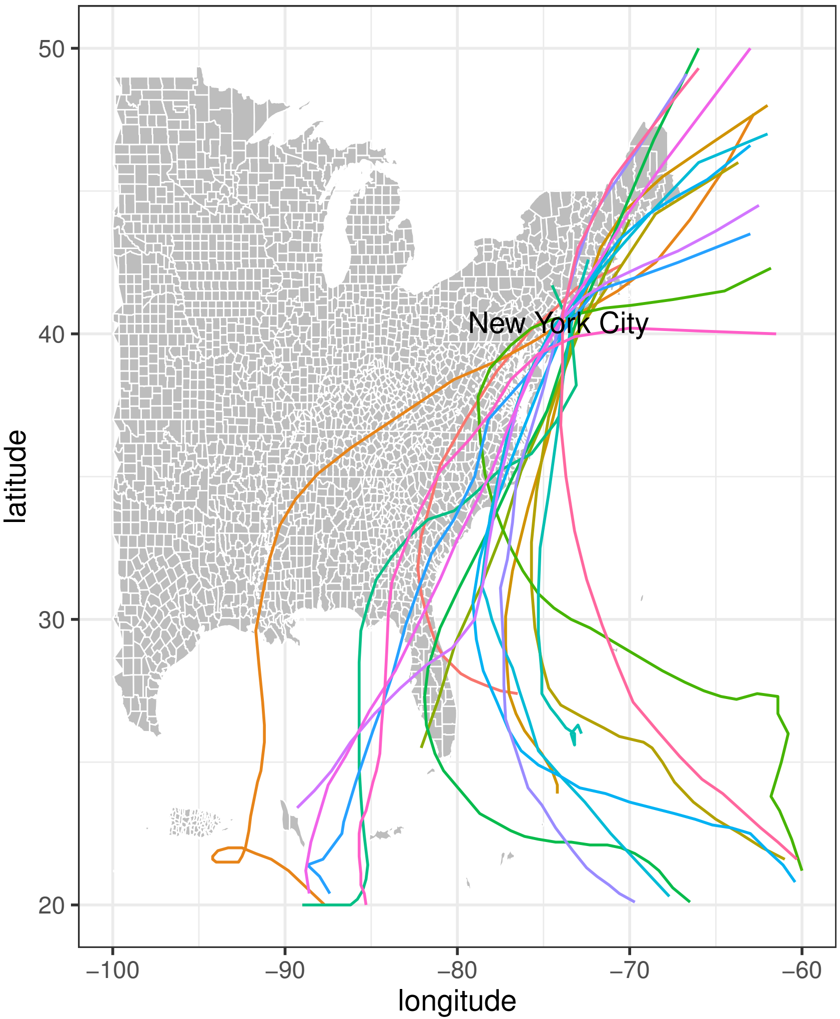
New York City
latitude
longitude
50
40
30
20
−100
−90
−80
−70
−60
(a)

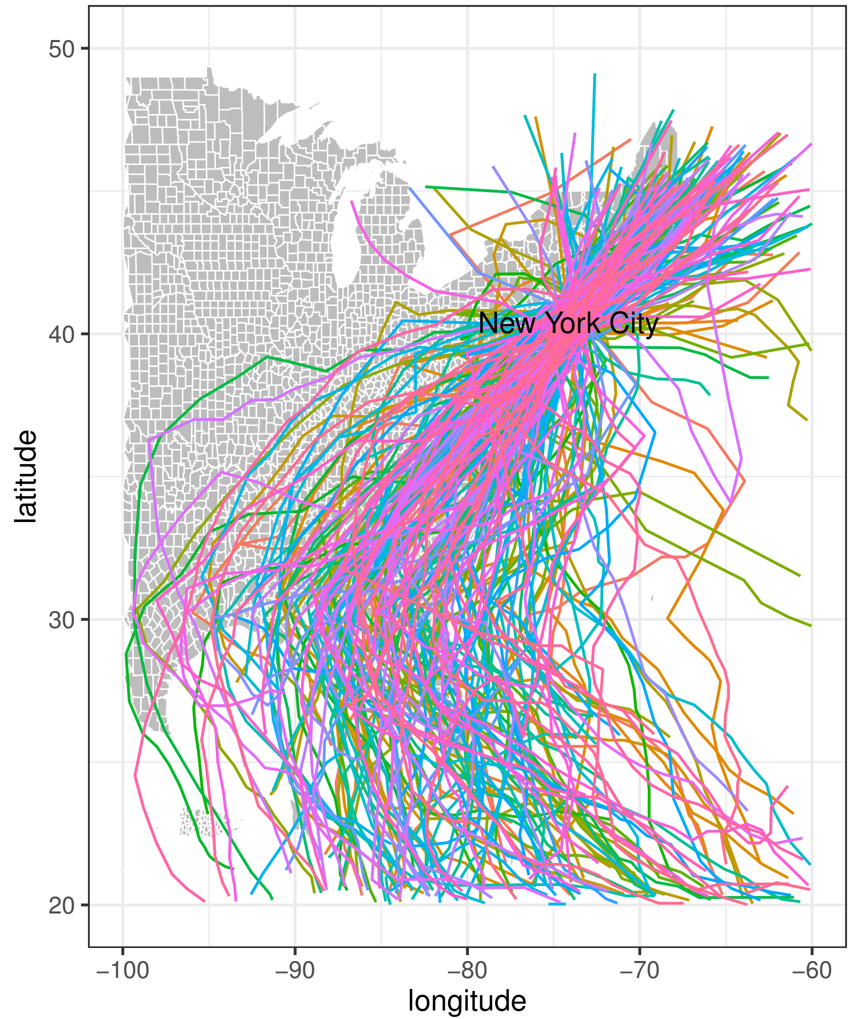
New York City
latitude
longitude
50
40
30
20
−100
−90
−80
−70
−60
(b)

Figure 11.

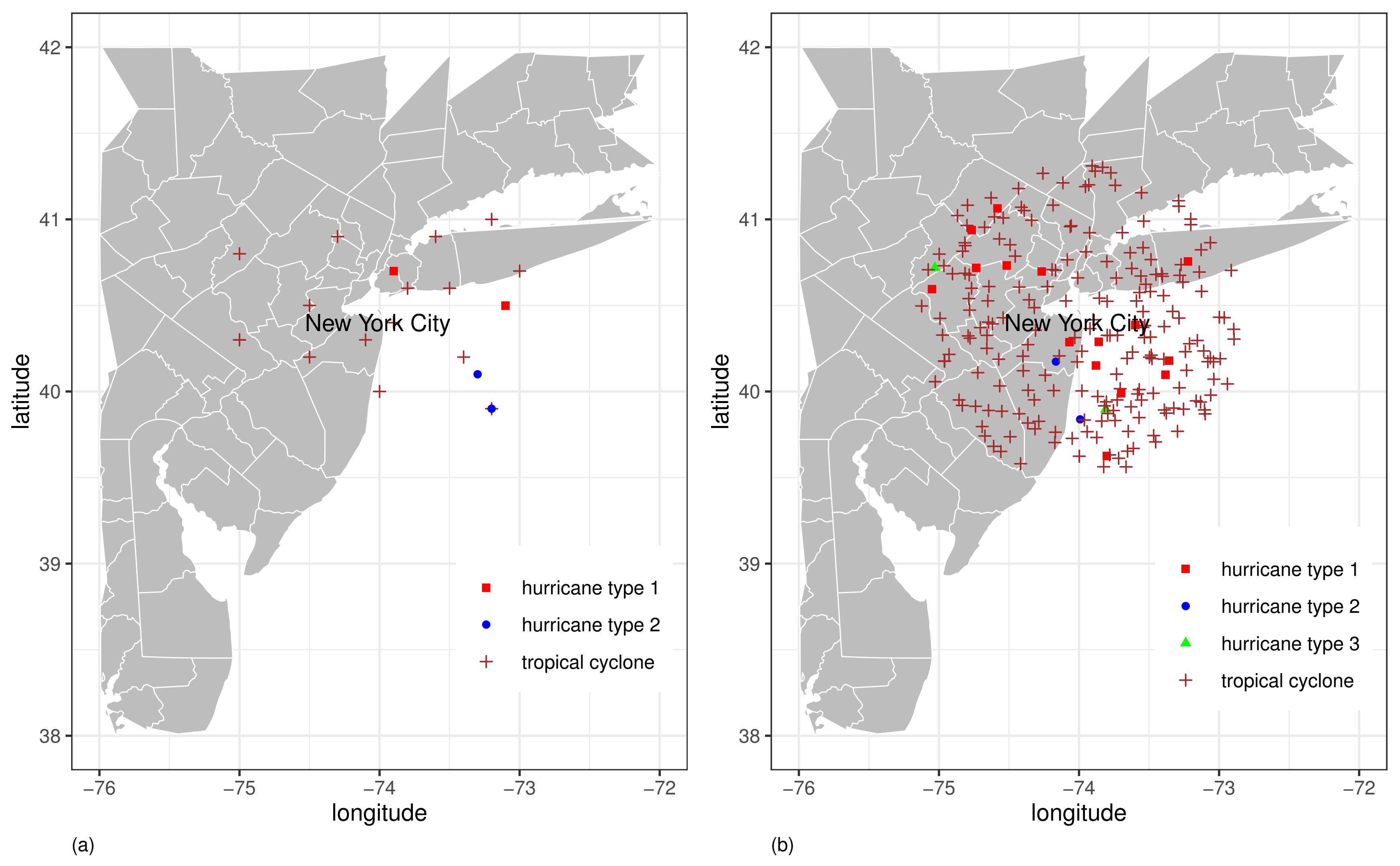

New York City
hurricane type 1
hurricane type 2
tropical cyclone
longitude
latitude
(a)
New York City
hurricane type 1
hurricane type 2
hurricane type 3
tropical cyclone
longitude
latitude
(b)

Figure 12.

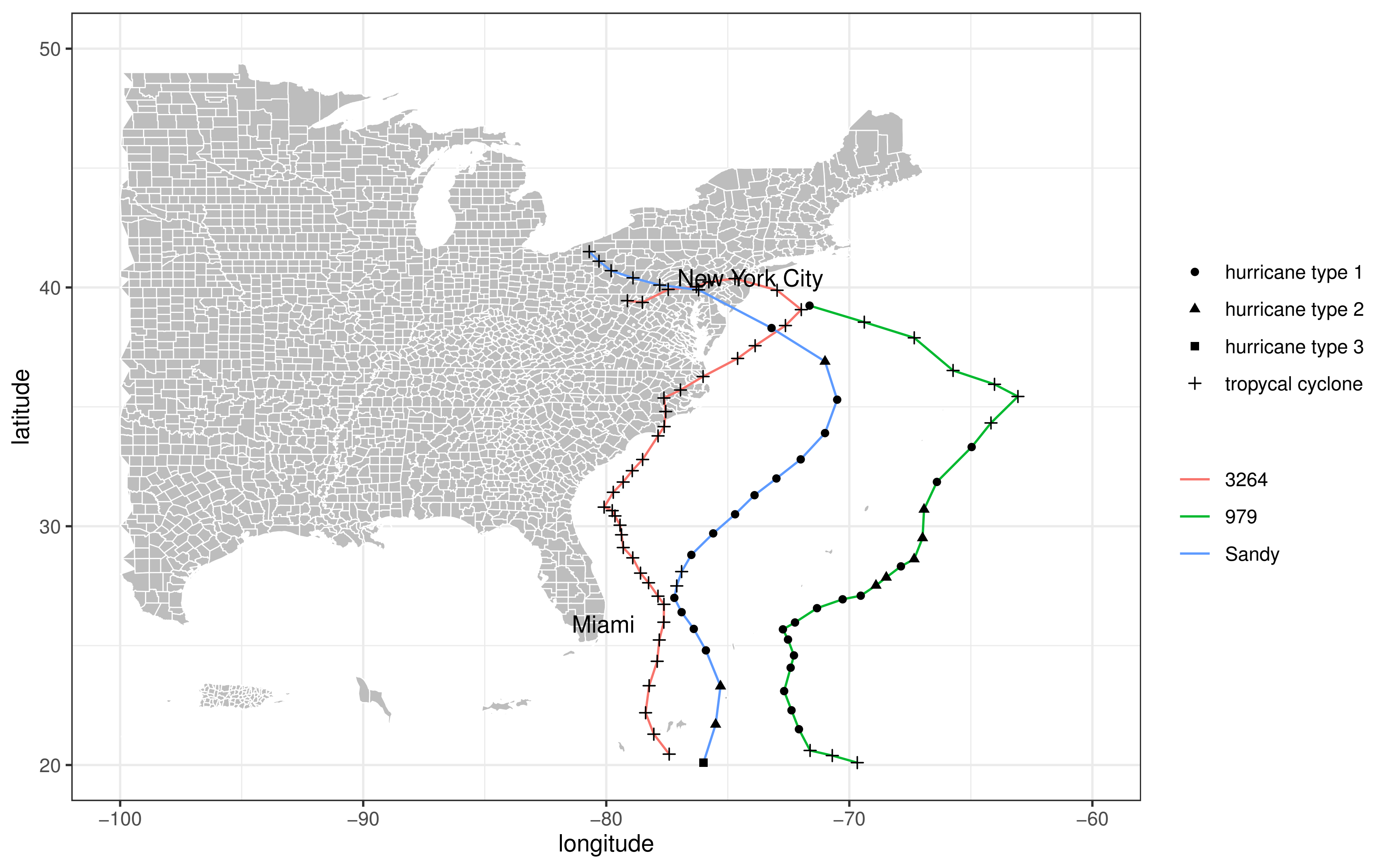
New York City
Miami
latitude
longitude
50
40
30
20
−100
−90
−80
−70
−60
hurricane type 1
hurricane type 2
hurricane type 3
tropycal cyclone
3264
979
Sandy

Figure 13-1.

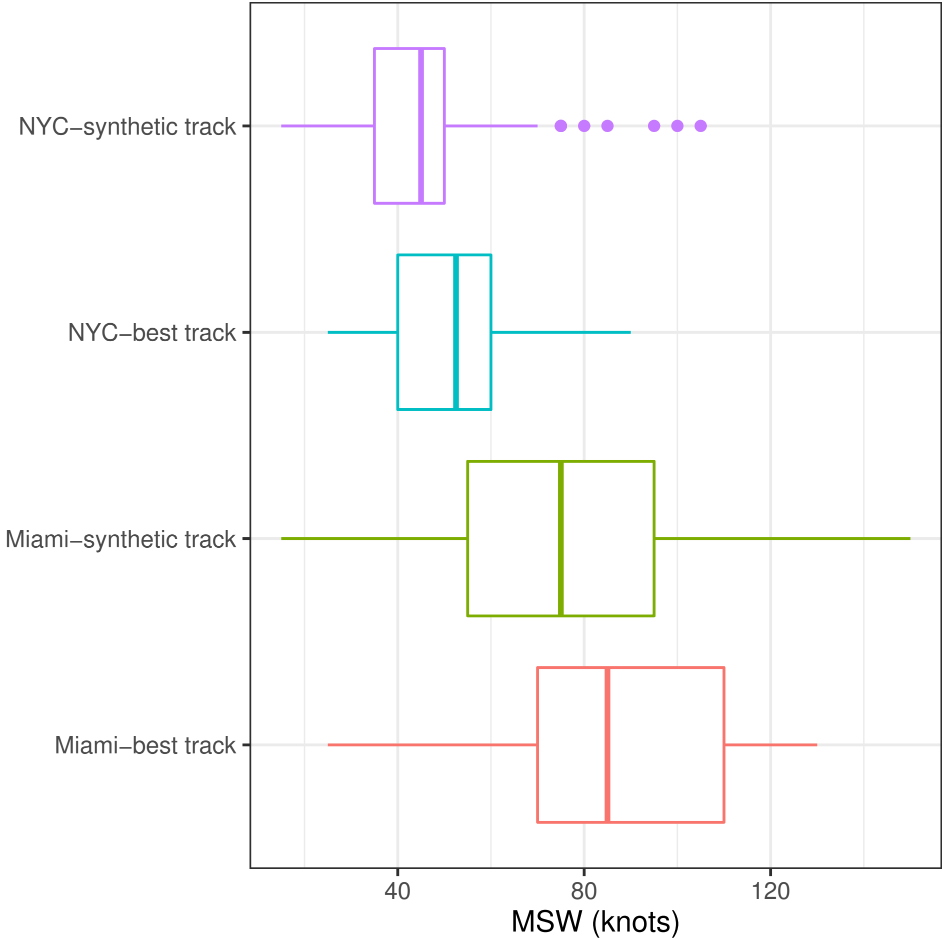
NYC−synthetic track
NYC−best track
Miami−synthetic track
Miami−best track
40
80
120
MSW (knots)

(a)

Figure 13-2.

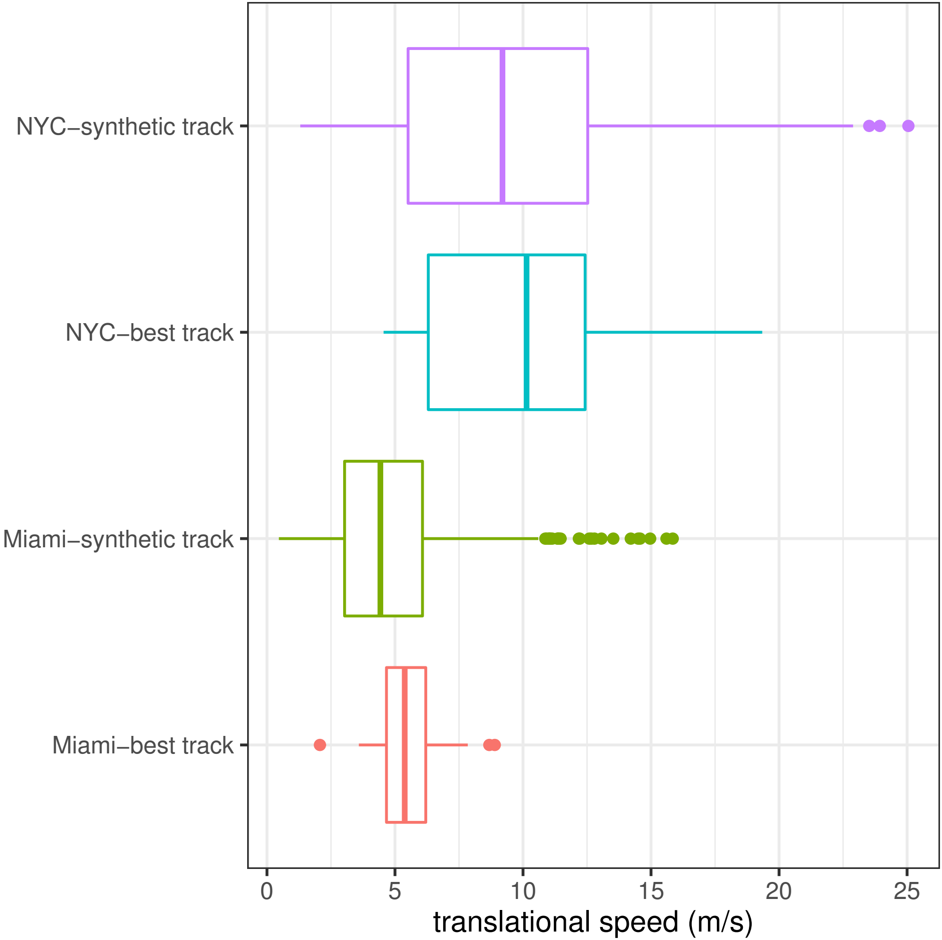
NYC–synthetic track
NYC–best track
Miami–synthetic track
Miami–best track
0
5
10
15
20
25
translational speed (m/s)

(b)